ELSEVIER

Coordination Chemistry Reviews 143 (1995)
35–69

COORDINATION CHEMISTRY REVIEWS

Confacial bioctahedral complexes of molybdenum and tungsten

Heinz-Bernhard Kraatz, P. Michael Boorman *

Department of Chemistry, University of Calgary, Calgary, Alta. T2N 1N4, Canada

Received 22 March 1994; in revised form 28 June 1994

Contents

* Corresponding author.

SSDI 0010-8545(94)07005-9

Abstract

The review deals with the chemistry of confacial bioctahedral or face-sharing bioctahedral (FBO) complexes of molybdenum and tungsten. As shown in the first section on bonding, complexes in which the metals are formally both in a +3 oxidation state are particularly stable owing to the optimal electronic configuration for the formation of metal–metal interactions. Hence the chemistry of such complexes is the most developed and is therefore most emphasized in the review. The fragment approach to bonding, introduced by Summerville and Hoffmann, is used to explain the structural features and reactivity of the FBO complexes. Tabulated data on many of the known complexes are provided, organized by the oxidation states of molybdenum and tungsten respectively. A brief review of the synthetic approaches, especially to M(III)–M(III) systems, is followed by a more lengthy discussion of the reactivity patterns that are emerging. These include interconversion between FBO and other structural types, especially edge-sharing bioctahedral (EBO) complexes, ligand site exchange reactions and ligand displacement reactions. Some relatively recent chemistry involving reactions of the coordinated ligands is then discussed, followed by a brief excursion into the known redox chemistry of the M(III)–M(III) systems which can lead to mixed oxidation state complexes. Finally, the possibility of developing catalytic uses for FBO complexes is suggested. The review cites 88 references to original papers and previous review articles. It deliberately avoids extensive discussion of aspects of the field which have been reviewed elsewhere in recent years.

Keywords: Confacial bioctahedral complexes; Molybdenum; Tungsten; Catalysis

---

List of abbreviations

EBO	edge-sharing bioctahedral
FBO	face-sharing bioctahedral
HOMO	highest occupied molecular orbital
LUMO	lowest unoccupied molecular orbital
PNP	bis(triphenylphosphoranylidene)ammonium chloride, $\{[(C_6H_5)_3P=]_2N\}Cl$
THF	tetrahydrofuran, C_4H_8O
THT	tetrahydrothiophene, C_4H_8S

1. Introduction

The chemistry of binuclear metal complexes has developed as an integral part of the field of cluster chemistry, since in many instances metal–metal-bonded structures are involved. Both theoretical and synthetic aspects of binuclear and multinuclear complexes containing metal–metal bonds have been extensively reviewed [1–5]. For certain metals the formation of binuclear complexes is a dominant feature of their chemistry. Such is the case for molybdenum and tungsten, especially in the +3 oxidation state. The focus of this review will be face-sharing bioctahedral (FBO)

complexes of these metals. This is one of the three commonly occurring binuclear structures of metals octahedrally surrounded by six ligands. These three structural motifs are shown below:

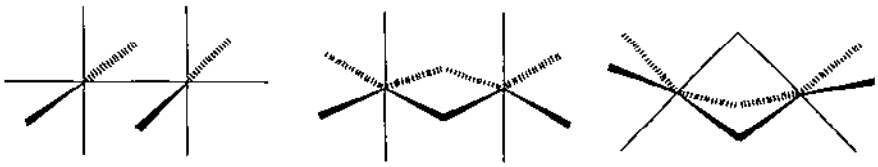

A B C

The two octahedra can be joined at a common vertex (**A**), at a common edge (**B**) or at a common face. The structures of edge-sharing bioctahedral (EBO) complexes have been reviewed [5]. Interconversion between types **B** and **C** has been observed in the presence of excess ligands and will be discussed later.

Binuclear complexes possessing a confacial bioctahedral framework (**C**) are encountered in both early and late transition metal chemistry and are especially prevalent in metal halide chemistry. The nonahalodimetallates have been reviewed recently [6].

This review will take the relatively narrow focus of Group 6 metals, especially molybdenum and tungsten, but comparisons with Nb and Ta FBO complexes will be made where appropriate. We will begin by examining the electronic structures of FBO complexes. The ensuing discussion of structural features is a logical second component of the review, since the variations in structure can be correlated with the bonding. An attempt will be made in Section 4 to rationalize the synthetic routes to FBO complexes. The discussion of reactivity of FBO complexes is of particular note (Section 5).

The reaction chemistry of FBO complexes has developed substantially over the last decade, but to date no attempt has been made to review this topic in detail. Face-sharing bioctahedra (FBOs) exhibit a fascinating array of reactivities, including ligand substitutions, equilibria between FBOs, edge-sharing bioctahedra (EBOs) and simple mononuclear complexes, and catalytic activities. The current interest in the application of molecular cluster complexes in catalysis is clearly a stimulus to the development of an understanding of the chemistry of these relatively simple binuclear systems. The discovery of the catalytic properties of Nb and Ta FBO complexes in alkyne polymerization and cyclotrimerization [7] prompted us to attempt analogous studies of Mo and W FBO complexes which will be discussed in Section 6 along with other likely future developments.

2. Bonding in confacial bioctahedral complexes

The variation in the structures and magnetic properties of $Cr_2Cl_9^{3-}$, $Mo_2Cl_9^{3}$ and $W_2Cl_9^{3-}$ has stimulated innumerable attempts to describe the electronic structures satisfactorily. Whereas $Cr_2Cl_9^{3-}$ has a Cr—Cr separation of 3.317(21) Å and is

paramagnetic, its tungsten analogue has a very short W—W separation (2.41(10) Å) and is diamagnetic. The $Mo_2Cl_9^{3-}$ ion has properties that are intermediate between those of its neighbours. Of prime importance in the evolution of theoretical treatments was the seminal paper by Cotton and Ucko [8]. They recognized that the metal–metal separation in FBO complexes and several other molecular parameters would be interrelated. These are shown in Fig. 1.

In an FBO complex with idealized D_{3h} symmetry and no interactions between the metal centres the d' and d'' distances will be equal. The angles β will be 70.53° and α will be 90°. The presence of interactions between the metal centres will result in deviations from these ideal values. In the case of metal–metal bonding the d'/d'' ratio will be less than unity, $\beta < 70.53°$ and $\alpha > 90°$. Repulsive metal–metal interactions will show the opposite effect. This phenomenological treatment does not explain why some complexes display metal–metal bonds while others do not. Molecular orbital descriptions are obviously required to fully explain the role of metal–metal bonding in FBO complexes and their influence on the magnetic behaviour of e.g. the $M_2X_9^{3-}$ ions of the Group 6 metals.

Several approaches have been taken in attempting to provide a theoretical basis for structural variations (e.g. the degree of M–M interactions) in FBO complexes. The simplest of these involves considering only the interacting metal d orbitals. The resulting energy level diagram (Fig. 2) has been frequently applied.

The strength of the metal–metal interaction will determine the HOMO–LUMO gap, which in turn will dictate the magnetic properties of these d^3–d^3 complexes. Thus a strong interaction will lead to diamagnetic complexes. Such is the case for the W(III)–W(III) systems.

Both qualitative and quantitative explanations of the electronic spectra and magnetic properties of the intermediate interaction Mo(III)–Mo(III) complexes have been given very successfully on this basis. Using the exchange-coupled pair model, Stranger et al. [9] were able to show that the antiferromagnetic exchange increases with a decrease in the length of the metal–metal vector. Dubicki et al. have provided a detailed analysis of features of the optical spectra of $Mo_2X_9^{3-}$ ions on the basis of

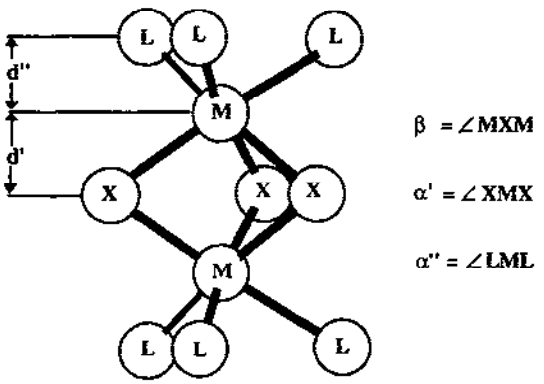

Fig. 1. A generalized confacial bioctahedron according to Cotton and Ucko. (Adapted from Ref. [8].)

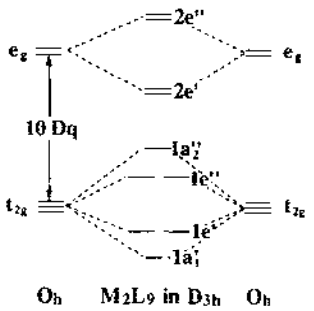

Fig. 2. Interaction of two octahedrally coordinated metal centres forming an FBO complex in D_{3h} point group symmetry.

this model [10]. Initially this involved states arising from $(t_{2g}^3)_a$–$(t_{2g}^2)_b$ interactions (a, b ≡ individual Mo centres) incorporating both metal–metal σ and π interactions as J_σ and J_π respectively. As expected, for many systems with short Mo—Mo distances J_σ was so large that the systems could be described without inclusion of these electrons in the exchange expressions. Conversely, for a complete description of some systems an extended model involving the single-ion e_g orbitals as well as the t_{2g} orbitals was found to be required [11]. Undoubtedly this model provides the most detailed description of the spectral transitions and magnetic properties, which treatments based on single-electron orbitals cannot match. However, generally the method is incapable of explaining variations in structure associated with changes in the ligands. An excellent summary of this and the work of others has been provided by Kazin et al. [6] and so this important aspect of FBO complexes will not be discussed in any further detail here. Rather, we wish to consider primarily the effect on the structures and chemistry of changes in the ligating atoms. Whole molecule descriptions have been used by several groups of investigators [12–14], but these in general underestimated the ligand contribution to the bonding in the bridging region [15]. The most successful descriptions have been provided by the fragment approach. Summerville and Hoffmann [15] were able to rationalize many of the known experimental facts using simple Hückel calculations and provided predictions about the structures of complexes for which no experimental data existed. Other workers have adopted the same approach, even though the computational methodologies may differ. We will therefore focus on this approach. The bonding in the FBO framework is considered in terms of the interaction between an M_2L_6 and an L_3 bridging fragment in D_{3h} point group symmetry (Fig. 3).

The M_2L_6 fragment is itself developed from two pyramidal ML_3 fragments interacting. The metal orbitals used for the formation of M—M bonds were shown to be very dependent on the nature of the terminal ligands L. An ML_3 fragment with π (e.g. Cl^-) or σ (e.g. H^-) donor ligands will be able to interact with any fragment approaching along the threefold axis owing to a tilt of the metal d orbitals towards this axis. A larger orbital tilt will allow a more directional interaction of the two ML_3 fragments, resulting in a metal–metal π-type interaction. Conversely, a smaller

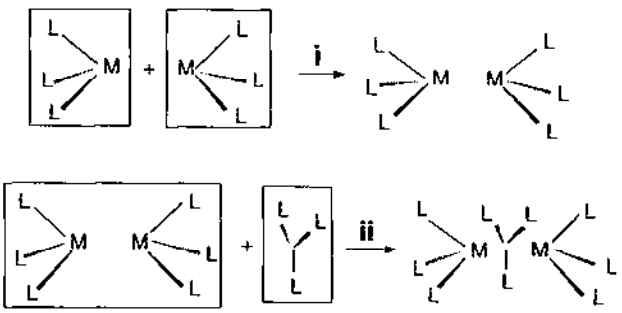

Fig. 3. Summerville and Hoffmann's fragment approach [15] to FBO complexes.

tilt will result in orbitals with more δ character. The partial orbital manifold for the M_2L_6 fragment is shown in Fig. 4.

The four groups of orbitals derive (in order of increasing energy) from (a) metal–metal bonding between d orbitals, (b) metal–metal antibonding between d orbitals, (c) metal–metal bonding between orbitals that are M—L antibonding in origin and (d) metal–metal antibonding between orbitals that are M—L antibonding in nature. (It is immediately obvious that the nature of the terminal ligands will affect the ultimate bonding pattern.)

The interaction between these orbitals and the L_3 (bridging ligand) set is very dependent on the nature of these ligands. For halide ions, commonly encountered in known complexes, the ligands have π donor characteristics. There will be nine combinations derived from the ligand p orbitals and three from the s orbitals. Since the latter are not important in the ensuing arguments, only the nine fully occupied p combinations are shown in Fig. 5.

The final step of combining the two fragments M_2L_6 and L_3 is represented in Fig. 6. The interaction of the populated bridge orbitals of the L_3 fragment with the metal–metal bonding orbitals of the M_2L_6 fragment (which are occupied in the case of Group 5 and 6 metals) will be repulsive in nature and thereby push up the energy of these metal–metal bonding orbitals. The magnitude is governed by the extent of the interaction between the bridge orbitals (designated as ^{b}) and the metal fragment.

The strongest interaction will be between the six metal–ligand antibonding orbitals of the M_2L_6 fragments and the bridge. These antibonding orbitals will thereby become populated, resulting in a weakening of the bond between the metal and the terminal ligands. The population of the M—M bonding orbitals by the interactions $2a_1' + 1a'^{b}_{1}$ and $2e' + 2e'^{b}$ will strengthen the M—M bond. On the other hand, the interactions $2a_2'' + 1a_2''^{b}$ and $2e'' + 1e''^{b}$ will populate the M—M antibonding orbitals and hence weaken the M—M bond.

The interactions $1a_2'' + 1a_2''^{b}$ and $1e'' + 1e''^{b}$ will be much smaller in magnitude than the comparable interactions $2a_2'' + 1a_2''^{b}$ and $2e'' + 1e''^{b}$ owing to the nodal characteristics of the metal-based orbitals. This means that these three metal–metal antibonding orbitals will contribute only very little to the overall M_2L_6 bridge bonding and therefore will remain virtually the same as in the M_2L_6 fragment. However, these

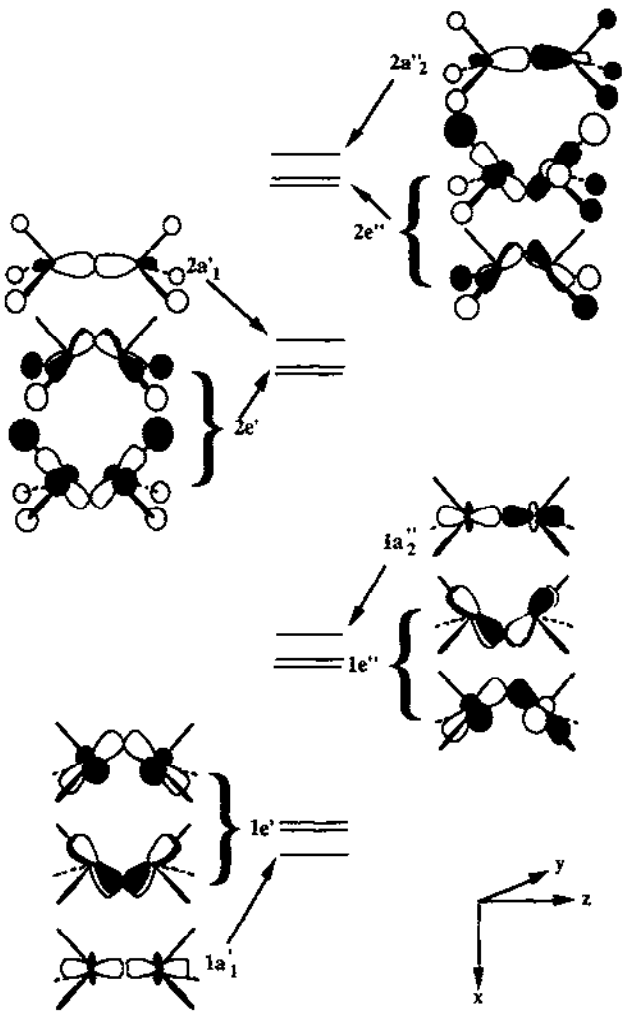

Fig. 4. Schematic representation of a partial orbital manifold of an M_2L_6 fragment in D_{3h} point group symmetry. (Adapted from Ref. [15].)

orbitals may be populated owing to the repulsive interactions (four-electron–two-orbital interactions) of the M—M bonding orbitals $1a_1'$ and $1e'$ with the bridge orbitals $1a_1'^{b}$ and $1e'^{b}$ (Fig. 7).

The interaction between the metal $1e'$ and the bridge $1e'^{b}$ is particularly important. For a weak interaction between the orbitals, e.g. as a result of a large metal–metal separation, the repulsive interaction between these sets of orbitals will be small. For a medium interaction between the metal and the bridge fragment the two orbitals in the e' representation ($1e'-1e'^{b}$) will be close in energy to the two M—M antibonding orbitals $1e''$. This small energy gap will give rise to the antiferromagnetic behaviour described above and partial population of the metal $1e''$ (strongly M–M

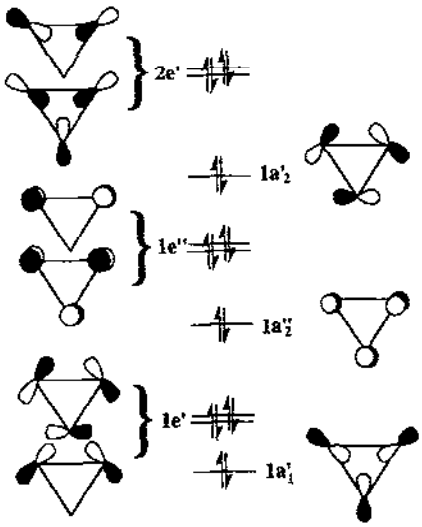

Fig. 5. Schematic partial orbital diagram of the L_3 fragment for π donors in D_{3h} point group symmetry (Adapted from Ref. [15].)

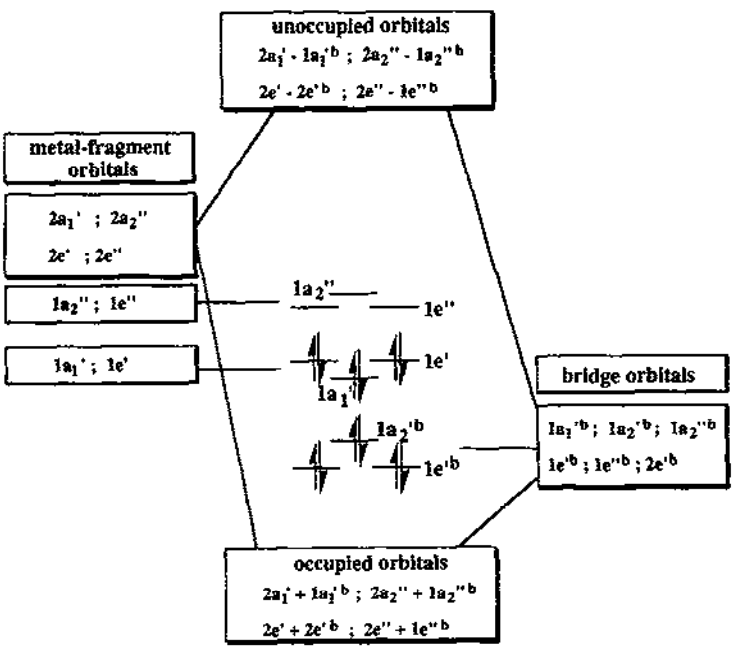

Fig. 6. Schematic interaction diagram for the two fragments M_2L_6 and L_3. (Adapted from Ref. [15].)

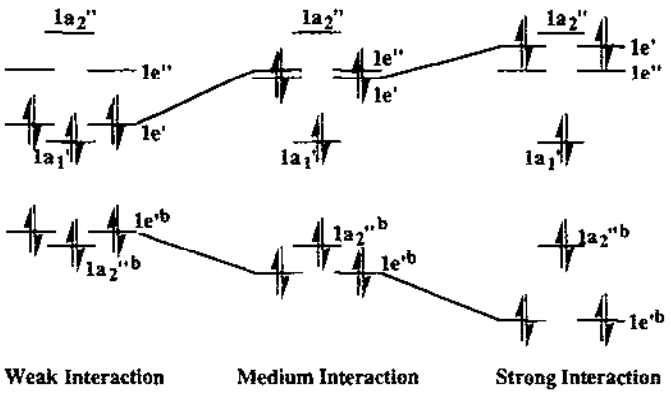

Fig. 7. Interactions between the metal 1e' orbitals and the filled bridge 1e' ($1e'^{b}$) orbitals for a d^3–d^3 system. (Adapted from Ref. [15].)

antibonding) orbitals will lead to a weakening of the M–M interaction and therefore an elongation of the M···M bond.

It will be recognized that the energy level diagrams ultimately produced are much like the t_{2g}-derived manifold in Fig. 2 and from the point of view of the magnetic properties they will still be dependent upon the e'–e" gap. However, the method of derivation now provides a basis for explaining the roles of the ligands in establishing this gap. This result will be used later in this article to explain structural and reactivity differences.

In the following we will take a closer look at mixed valence FBO complexes. For this discussion it will be sufficient to consider the simplified bonding picture as can be obtained by considering the interaction of the d orbitals of the two metal centres in an octahedral field (see Fig. 2) [6,16]. In fact, we can concentrate on the lower manifold stemming from the interaction of the t_{2g} sets of the O_h metal centres. For further discussion the correlation between D_{3h} and C_{2v} symmetry, as shown in Fig. 8, also has to be considered.

$1a_1$ represents a metal–metal σ bond, while $2a_1$ and $1b_2$ are π or δ bonding with respect to the metals. $1b_1$ and $1a_2$ are the M−M π* or σ* orbitals and $2b_1$ is the M−M σ* orbital. As noted earlier, for M_2L_9 systems with the d^3–d^3 configuration the bonding orbitals are fully occupied. We now consider mixed valence systems, e.g. d^2–d^3 systems, which are sometimes encountered for tungsten [17,18]. In this

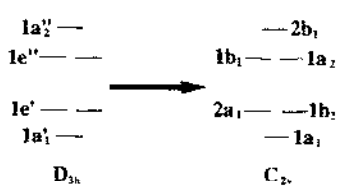

Fig. 8. Correlation diagram between the partial orbital manifold of an FBO complex in D_{3h} and C_{2v} point group symmetries.

case five electrons occupy the metal–metal bonding levels ($1a_1$ (σ), $2a_1$ and $1b_2$ (π/δ)). A geometrical distortion other than an elongation of the metal–metal bond will lift the degeneracy of the two orbitals in question (Jahn–Teller distortion) (see Fig. 9). Hence a distortion of the FBO framework will be energetically stabilizing.

For $(^iPr_4N)_2[W_2Br_9]$ a distortion from ideal D_{3h} symmetry of the dianion was observed by Templeton et al. [17]. In the Cotton and Ucko description [8] of the FBO framework the three planes used to define the parameters d' and d'' are assumed to be perpendicular to the metal–metal vector. However, in the case of the $[W_2Br_9]^{2-}$ dianion a rotation of the two planes defined by the terminal bromine atoms by 3° towards one of the bridging bromine atoms (Br*) is observed as shown in Fig. 10a. This distortion leads to the removal of the degeneracy of the two π/δ bonding orbitals $2a_1$ (Fig. 10b) and $1b_2$ (Fig. 10c). In the case of the $2a_1$ orbital (Fig. 10b) a rotation of the two planes towards the bridgehead bromine will rotate the metal orbitals ($\sqrt{\frac{2}{3}}d_{x^2-y^2}+\sqrt{\frac{1}{3}}d_{xy}$) towards each other and so reduce their directionality and increase the δ character of the orbital. This orbital will be raised in terms of energy. As shown in Fig. 10c, the rotation will increase the directionality of the two $\sqrt{\frac{2}{3}}d_{yz}+\sqrt{\frac{1}{3}}d_{xz}$ orbitals of the metals and thereby stabilize the $1b_2$ molecular orbital (MO) of the FBO complex. This will lead to an increase in the orbital's π character. The σ bond is not influenced by this distortion.

Another way to remove the degeneracy of the two orbitals will be a distortion in

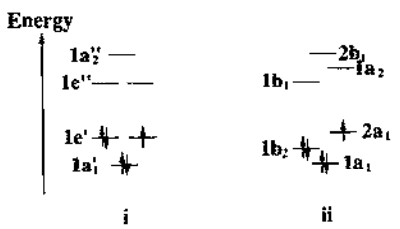

Fig. 9. Effects of a geometrical distortion of the FBO framework on the orbital manifold of a d^3–d^2 FBO complex: (i) undistorted D_{3h} point group symmetry; (ii) distorted C_{2v} point group symmetry.

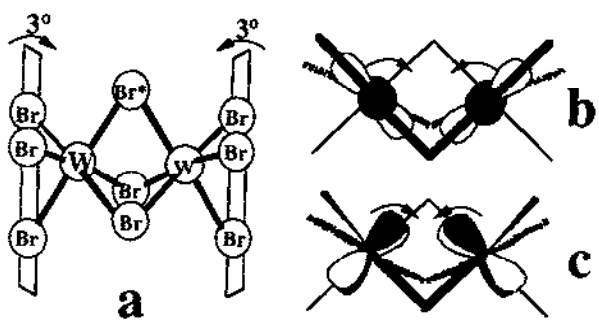

Fig. 10. Canting of the two planes defined by the terminal bromine atoms towards Br* by 3° (a). This will remove the degeneracy between the two orbitals $2a_1$ (b) and $1b_2$ (c). The contributions from the ligands to the two orbitals have been omitted for clarity. (Adapted from Ref. [17].)

the bridging region. Moving two ligands closer together will increase the splitting between $4a_1 - 2a_1^b$ and $2b_2 - 1b_2^b$. (These are the C_{2v} components of $1e'^b$ and $1e'$ shown in Fig. 6 for D_{3h} symmetry.) For d^2–d^2 and d^3–d^2 systems this distortion will result in a net stabilization. However, for d^3–d^3 systems a distortion of the bridge will not result in an energy gain.

A distortion of the bridging region is quite common and has been observed for mixed valence systems [18] as well as for Group 5 d^2–d^2 systems [19].

Although the preceding MO analysis helps in understanding the bonding qualitatively (see Fig. 6), there is still ambiguity about the question of metal–metal multiple bonding in systems such as $Mo_2Cl_9^{3-}$ and $W_2Cl_9^{3-}$. Summerville and Hoffmann [15] have described $Mo_2Cl_9^{3-}$ as being intermediate between $Cr_2Cl_9^{3-}$ with no M···M bond and $W_2Cl_9^{3-}$ with a W—W triple bond. However, recent results by Dubicki et al. [10] suggest that there are no fundamental differences between the bonding in $Mo_2Cl_9^{3-}$ and $W_2Cl_9^{3-}$. In both systems a strong M···M σ bond exists. The π interactions in the two systems are considered weak, with those in the Mo complex being weaker.

In fact, a comparison of the structural parameters of isocationic systems shows that the variations in M—M bond lengths and bond angles are rather small, indicating a similar bonding situation (see Table 1). This is even more pronounced for the two thioether-bridged Group 5 systems $(THT)Br_2Nb(\mu\text{-}Br)_2(\mu\text{-}THT)NbBr_2(THT)$ and $(THT)Br_2Ta(\mu\text{-}Br)_2(\mu\text{-}THT)TaBr_2(THT)$, described by Templeton et al. [17] as possessing an M—M double bond (see Table 1).

It has been observed that upon the introduction of a μ-hydride the M···M bond distance decreases significantly compared with $(\mu\text{-}Cl)_3$ in the case of M ≡ Mo [20]. Electronic factors are believed to be responsible for this effect. The interaction between the occupied metal–metal bonding orbitals of the M_2L_6 fragment and the occupied orbitals of the L_3 bridge fragment will be repulsive in nature, since it is a four-electron–two-orbital interaction [15]. The interaction of the $1a_1'$ orbital of the M_2L_6 fragment with the $1a_1'^b$ orbital of the bridge (see Fig. 6) can be viewed as being responsible for the structural changes. The p orbital combination used by a Cl_3 fragment (Fig. 11a) will differ from the s orbital combination of H_3 in its interactions with the metal $1a_1'$ orbital.

Table 1
Structural parameters for M_2L_9 systems, comparing isostructural Nb and Ta systems and Mo and W systems

Complex	M–M (Å)	M–X–M (°)	M–S–M (°)
$Cs_3Mo_2Cl_9$[a]	2.66	64.5	
$Cs_3W_2Cl_9$[a]	2.50	61.4	
$K_3Mo_2Cl_9$[a]	2.52	60.6	
$K_3W_2Cl_9$[a]	2.41	58.1	
$(THT)Br_2Nb(\mu\text{-}Br)_2(\mu\text{-}THT)NbBr_2(THT)$[b]	2.728(5)	62.5[c]	66.5(3)
$(THT)Br_2Ta(\mu\text{-}Br)_2(\mu\text{-}THT)TaBr_2(THT)$[b]	2.710(2)	62.0[c]	69.0(3)

[a] From Ref. [10]; [b] from Ref. [17]; [c] arithmetic mean of the two M–Br–M bond angles.

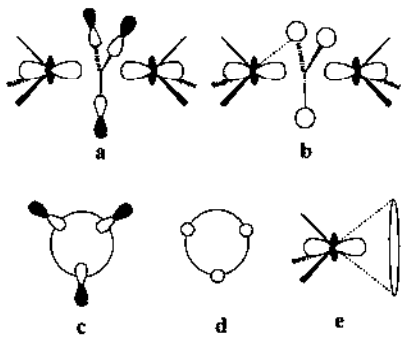

Fig. 11. Interaction of the filled $1a_1'$ orbital of the M_2L_6 fragment with the filled $1a_1'^{b}$ orbital of the L_3 fragment, showing the difference in phase relationships with the metal-based orbital between a set of p donating orbitals (a) and s donating orbitals (b); see text. (Adapted from Ref. [15].)

The circle (indicated in Fig. 11e) represents a phase reversal due to the nodal characteristics of the metal d_{x^2} orbital. Since the interaction of the L_3 fragment with the M_2L_6 fragment is repulsive in nature, a geometry minimizing this repulsive interaction will be the most stable. For chloride to reach a minimum interaction with the M_2L_6 fragment, it has to move outwards (Fig. 11c), leading to a more acute angle M—(μ-Cl)—M. One might think that this will bring the metal centres closer together; however, owing to the population of the M—M antibonding orbitals, these get pushed apart to reduce interaction. For the simple s σ donor, hydride, the M—(μ-H)—M angle will be close to 70°, since now the overlap between the three 1s orbitals of the hydride and the $1a_1'$ orbital of the M_2L_6 fragment will be close to zero (Fig. 11d). In addition, the overall repulsive interaction will be less for hydrides than for chlorides, allowing an overall closer M—M distance.

In summary, the two approaches to describing the electronic structure of M_2L_9 complexes are each useful in certain respects. The simplified, metal-based d orbital description normally used in the exchange-coupled pair model provides an excellent analysis of the magnetic and spectral properties. It also gives a basis for assigning metal–metal bond orders. However, to rationalize the effects of both the terminal and bridging ligands on the geometry and reactivity of FBO complexes, the fragment approach to generating an MO description is preferable.

3. Molecular structure

A brief structural overview of known FBO complexes of molybdenum and tungsten is presented in Tables 2 and 3. As can be seen, FBO complexes are formed by Group 6 metals in oxidation states from III to V with a strong preference for M(III)–M(III) binuclear complexes. For molybdenum it will be noted that Mo—Mo separations are variable and strongly dependent on the nature of the coordinated ligands. For tungsten there is a clear trend. The higher the formal oxidation state of the metals in the FBO complexes, the larger are the M—M separations.

Table 2
Confacial bioctahedral dimolybdenum complexes

Complex	Oxidation state	d(M–M) (Å)	Ref.
$(Et_3P)Cl_2Mo(\mu\text{-}Cl)_3MoCl(PEt_3)_2$	III–III	2.815	[21]
$(PhMe_2P)Cl_2Mo(\mu\text{-}Cl)_3MoCl_2(PMe_2Ph)_2$	III–III	2.658	[22]
$(Et_3P)Cl_2Mo(\mu\text{-}Cl)_3MoCl_2(PEt_3)_2{\cdot}CH_2Cl_2$	III–III	2.753	[22]
$(Ph_4P)[(Me_2S)Cl_2Mo(\mu\text{-}Cl)_3MoCl_2(SMe_2)]$	III–III	2.746	[23]
$(Me_2S)Cl_2Mo(\mu\text{-}SMe_2)(\mu\text{-}Cl)_2MoCl_2(SMe_2)$	III–III	2.462	[23]
$(THT)Cl_2Mo(\mu\text{-}THT)(\mu\text{-}Cl)_2MoCl_2(THT)$	III–III	2.470	[24]
$(THT)Cl_2Mo(\mu\text{-}Cl)_3MoCl(THT)_2$	III–III	2.689	[24]
$Cs_3[Cl_3Mo(\mu\text{-}Cl)_3MoCl_3]$	III–III	2.655	[25]
$Cs_3[Cl_3Mo(\mu\text{-}H)(\mu\text{-}Cl)_2MoCl_3]$	III–III	2.380	[26]
$(PyH)_3[Cl_3Mo(\mu\text{-}H)(\mu\text{-}Cl)_2MoCl_3]$	III–III	2.371(1)	[27]
$Cs_3[Cl_3Mo(\mu\text{-}H)(\mu\text{-}Cl)_2WCl_3]$[a]	III–III	2.445(3)	[28]
$\{Me_3PH\}[syn\text{-}(Me_3P)Cl_2Mo(\mu\text{-}Cl)_3MoCl_2(PMe_3)]$	III–III	[b]	[29]
$\{Me_4P\}[syn\text{-}(Me_3P)Cl_2Mo(\mu\text{-}Cl)_3MoCl_2(PMe_3)]$	III–III	2.694	[29]
$\{Me_3PH\}[gauche\text{-}(Me_3P)Cl_2Mo(\mu\text{-}Cl)_3MoCl_2(PMe_3)]$	III–III	2.717	[29]
$Cs_3[Br_3Mo(\mu\text{-}Br)_3MoBr_3]$	III–III	2.816	[25]
$Cs_3[Br_3Mo(\mu\text{-}H)(\mu\text{-}Br)_2MoBr_3]$	III–III	2.439	[26]
$(PhMe_2P)I_2Mo(\mu\text{-}I)_3MoI_2(PMe_2Ph)_2$	III–III	2.909	[30]
$(PhMe_2P)Br_2Mo(\mu\text{-}Br)_3MoBr_2(PMe_2Ph)_2$	III–III	2.749	[30]
$(Ph_4As)[(Me_3P)I_2Mo(\mu\text{-}I)_3MoI_2(PMe_3)]$	III–III	3.022	[31]
$(py)(^iPrO)_2Mo(\mu\text{-}CO)(\mu\text{-}O^iPr)_2Mo(O^iPr)_2(py)$	III–III	2.495	[32]
$[(Me_2NH)(^iPrO)_2Mo(\mu\text{-}O^iPr)_3Mo(^iPrO)_2(Me_2NH)]^-$	III–III	2.601	[33]
$(Ph_4P)[Mo_2O_2(\mu\text{-}N_3)(S(CH_2)_3S)_3]$	V–V	2.893	[34]
$(Et_4N)[Mo_2O_2(SCH_2CH_2O)Cl_3]$	V–V	2.728	[35]
$(Et_4N)[Mo_2O_2(SCH_2CH_2O)_3Cl]$	V–V	2.731	[35]
$(Pr_3NH)[Mo_2O_2(SCH_2CH_2O)_3(SCH_2CH_2OH)$	V–V	2.739	[35]
(dedtc)OMo(μ-Cl)(μ-SPh)$_2$MoO(dedtc)[$MoOCl_4(OH_2)$]	V–V	2.822	[36]
$(HNEt_3)[Mo_2(NNC_6H_5)_4(SC_6H_5)_5]$	V–V	3.527	[37]

[a] This mixed metal complex is included for comparison; [b] two independent formula units are found in the unit cell, with d(Mo–Mo) = 2.763(2) and 2.713(2) Å.

W(III)–W(III) complexes have short W—W separations ranging between 2.419 and 2.485 Å. For W(III)–W(IV) systems W—W bonds ranging from 2.505 to 2.519 Å have been found. For W(IV)–W(IV) and W(V)–W(V) the metal–metal separations are 2.438–2.564 and 2.655–2.888 Å respectively. For systems with heavier halides the M—M separation increases, probably as a result of the ligand size.

FBO complexes have been obtained with ligands ranging from π acids such as CO and phosphines to strong π donors such as halides and pseudohalides. All $M_2X_6(PR_3)_3$ systems (M ≡ Mo, W; X ≡ halide) possess three terminal phosphine ligands and μ-halide bridges. Owing to the repulsive nature of the M–halide–M interaction (see Section 2), long metal–metal bond lengths are common for Mo(μ-X)$_3$Mo systems. However, the Mo—Mo bond distance in d^3-d^3 systems is quite flexible and greatly influenced by the type of phosphine ligand and even crystal-packing forces. An example of the crystal-packing effect is the difference in Mo—Mo

Table 3
Confacial bioctahedral ditungsten complexes

Complex	Oxidation state	d(M—M) (Å)	Ref.
$K_3[Cl_3W(\mu\text{-}Cl)_3WCl_3]$	III–III	2.418	[38,39]
$\{Ph_4P\}[(THF)Cl_2W(\mu\text{-}Cl)_3WCl_2(THF)]$	III–III	2.409	[40]
$\{(THF)_3Na\}[(THF)Cl_2W(\mu\text{-}Cl)_3WCl_2(THF)]$	III–III	2.403	[41]
$(PEt_3)Cl_2W(\mu\text{-}Cl)_3WCl(PEt_3)_2\cdot CH_2Cl_2$	III–III	2.471	[42]
$(Me_2PhP)Cl_2W(\mu\text{-}Cl)_3WCl(PMe_2Ph)_2$	III–III	2.443	[43]
$\{Ph_4P\}[Cl_3W(\mu\text{-}H)(\mu\text{-}SMe_2)_2WCl_3]$	III–III	2.419	[44]
$\{(PhCH_2)(CH_3)_2S\}[Cl_3W(\mu\text{-}Cl)(\mu\text{-}SMe_2)_2WCl_3]$	III–III	2.477	[45]
$Cl_3W(\mu\text{-}SEt_2)_3WCl_3\cdot MeCN$	III–III	2.499	[46]
$\{Me_3S\}[Cl_3W(\mu\text{-}Cl)(\mu\text{-}SMe_2)WCl_3]$	III–III	2.475	[46]
$\{(THF)_3Na\}[Cl_3W(\mu\text{-}SEt_2)_2(\mu\text{-}SEt)WCl_3]$	III–III	2.474	[47]
$\{Ph_4P\}[Cl_3W(\mu\text{-}THT)(\mu\text{-}S(CH_2)_4Cl)WCl_3]$	III–III	2.485	[47]
$\{Ph_4P\}_2[Cl_3W(\mu\text{-}Cl)(\mu\text{-}SEt)(\mu\text{-}SEt_2)WCl_3]$	III–III	2.442	[48]
$(Me_2PhP)Br_2W(\mu\text{-}Br)_3WBr(PMe_2Ph)_2$	III–III	2.477	[43]
$[HPEt_3]^+[W_2Cl_7(PEt_3)_2]$	III–III	2.438	[49]
$\{PNP\}_2[Cl_3W(\mu\text{-}Cl)_3WCl_3]$	III–IV	2.540	[39]
$\{Ph_4P\}[Cl_3W(\mu\text{-}Cl)_3WCl_2(THF)]$	IV–III	2.520	[40]
$(Me_2S)Cl_2W(\mu\text{-}SEt)_3WCl_2(SMe_2)$	IV–III	2.505	[18]
$\{Ph_4As\}_2[Cl_3W(\mu\text{-}Cl)(\mu\text{-}SPh)_2WCl_3]\cdot 1.4CH_2Cl_2$	IV–III	2.519	[50]
$\{^nPr_4N\}_2[Br_3W(\mu\text{-}Br)_3WBr_3]$	IV–III	2.601	[17]
$\{Ph_4P\}_2[Cl_3W(\mu\text{-}Se)(\mu\text{-}SePh)_2WCl_3]\cdot 2CH_2Cl_2$	IV–IV	2.564	[51]
$(cC_5H_9{-}O)_3W(\mu\text{-}H)(\mu\text{-}O{-}cC_5H_9)W(O{-}cC_5H_9)(NHMe_2)$	IV–IV	2.438	[52]
$(Me_2S)Cl_2W(\mu\text{-}S)(\mu\text{-}SEt)_2WCl_2(SMe_2)$	IV–IV	2.526	[53]
$\{Ph_4P\}_2[Cl_3W(\mu\text{-}S)(\mu\text{-}SEt)_2WCl_3]$	IV–IV	2.522	[53]
$(RO)_3W(\mu\text{-}CH{-}ptol)(\mu\text{-}OR)_2W(O)(OR)(py)$[a]	V–V	2.655	[54]
$\{Ph_4P\}[Cl_2OW(\mu\text{-}Cl)(\mu\text{-}S^tBu)_2WOCl_2]$	V–V	2.854	[55]
$\{Ph_4As\}[Cl_2OW(\mu\text{-}Cl)(\mu\text{-}SC_6H_4CH_3\text{-}4)_2WOCl_2]$	V–V	2.882	[56]
$[(PCH_2Ph)Ph_3][Cl_2OW(\mu\text{-}Cl)_3WOCl_2]$	V–V	2.849	[57]
$[(PCH_2Ph)Ph_3][Cl_2(EtN)W(\mu\text{-}Cl)_3W(NEt)Cl_2]$	V–V	2.839	[57]
$[(PCH_2Ph)Ph_3][Cl_2(PhN)W(\mu\text{-}Cl)_3W(NPh)Cl_2]$	V–V	2.835	[57]

[a] $R \equiv CH_2{}^tBu$.

bond lengths in the anion $[syn\text{-}(Me_3P)Cl_2Mo(\mu\text{-}Cl)_3MoCl_2(PMe_3)]^-$ [29]. Changing the counter-ion from Me_3PH^+ to Me_4P^+ causes a dramatic decrease in the length of the Mo—Mo vector. Stranger et al. reported a similar cation dependence for $Mo_2X_9^{3-}$ [9]. For all crystallographically characterized phosphine complexes of the type $M_2X_6L_3$ only the anti isomer (C_{2v}) has been isolated. Fig. 12 shows the structure of one example of such a complex, $Mo_2Cl_6(PEt_3)_3\cdot CH_2Cl_2$, which was reported by Poli and Mui [22]. Interestingly, there are structural differences between this crystalline form of the complex and that reported by Cotton et al. [21].

Possibly owing to relativistic effects, the M—M separation in the tungsten FBO systems is largely invariant to the nature of the bridging ligand. For example, $\{Ph_4P\}[(THF)Cl_2W(\mu\text{-}Cl)_3WCl_2(THF)]$ [40], a complex with a strongly repulsive bridge, has a very short W—W separation (d(W—W) = 2.403 Å).

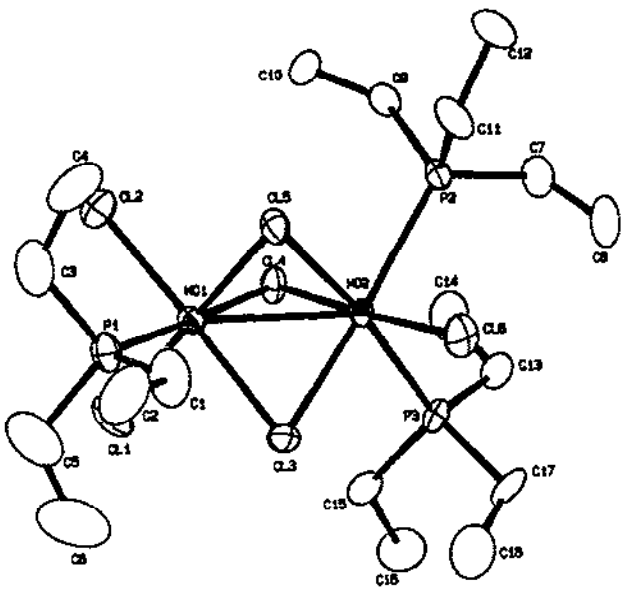

Fig. 12. ORTEP representation of $Mo_2Cl_6(PEt_3)_3$. (Reproduced with permission from Ref. [26].)

Thioether ligands can coordinate in bridging positions as well as in terminal positions. The M—S distance for the terminal thioether ligands in FBO complexes is longer than expected for an M—S single bond based on covalent radii. The $M-S_{bridge}$ distance is markedly shorter than the $M-S_{terminal}$ bonds. Templeton et al. [19] explained this in terms of steric interactions with the halogens. The terminal thioethers are hindered from approaching the metals any closer by the steric repulsion with the halogens. The bridging thioether, on the other hand, is not sterically hindered and can be close to the metal centre. The long $M-S_t$ bond would explain the lability of terminal thioethers. They are readily substituted by anionic donors such as halides [58] and other neutral ligands such as THF [59], leaving the bioctahedral framework unchanged. The bridging thioether, on the other hand, is not easily replaced by donor ligands and its replacement usually leads to the destruction of the confacial framework.

At this time it is worth pointing out that for all known Group 5 and 6 FBO complexes a thioether ligand in the bridging position causes the two metal centres to have short metal–metal contacts. For Mo systems the influence of the bridging ligand on the Mo—Mo separation has been demonstrated by Boorman and coworkers [23,24]. It is evident that the massive structural changes observed are closely related to the nature of the bridging ligand. For example, in the antiferromagnetic $[(Me_2S)Cl_2Mo(\mu\text{-}Cl)_3MoCl_2(Me_2S)]^-$ the two metals are separated by 2.746 Å, whereas in the diamagnetic thioether-bridged complex $(Me_2S)Cl_2Mo(\mu\text{-}Cl)_2(\mu\text{-}SMe_2)MoCl_2(Me_2S)$ the intermetallic distance is significantly shorter (2.462 Å) [23]. The thioether in the bridging position causes a strong interaction of the two molybdenum centres, as indicated by the shortening of the Mo—Mo bond and a change

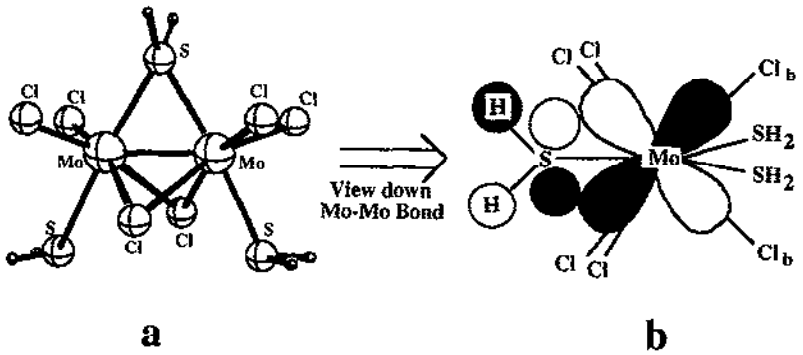

Fig. 13. (a) The model complex $(H_2S)Cl_2Mo(\mu\text{-}Cl)_2(\mu\text{-}SH_2)MoCl_2(SH_2)$. (b) The interaction between the σ^* orbital of the thioether and the metal d orbitals shown schematically, viewing down the Mo—Mo vector. The orbital contributions from the remaining ligands have been omitted for clarity. (Adapted from Ref. [60].)

in magnetic behaviour. In a density functional theoretical study [60] using the fragment approach described earlier, the bonding situations of model d^3–d^3 thioether-bridged FBO systems of the overall formulation $[Mo_2Cl_{9-n}(SH_2)_n]^{n-3}$ with $n=2$, 3, 4 and 5 as well as complexes $(SH_2)Cl_2Mo(\mu\text{-}Cl)_2(\mu\text{-}SR_2)MoCl_2(SH_2)$ with R≡H, F and Me were calculated and analysed. It was found that the availability of a low-lying σ^* orbital of the thioether allows a backbonding interaction with one of the metal–metal bonding orbitals (b_2 orbital). Fig. 13 shows this interaction.

The backbonding interaction removes some of the electron density from the metals, thereby allowing the metals to be closer together. Backbonding is of significantly less importance for terminal thioether ligands.

FBO complexes with three thioethers in the bridging region are known for Nb, Ta [61] and W [46]. These complexes possess a very short metal–metal separation, indicative of strong M—M bonding, which has been interpreted as an M—M triple bond. They also have short M—S_b bond lengths. Fig. 14 shows an ORTEP plot of $[Cl_3W(\mu\text{-}SEt_2)_3WCl_3]$ [46]. The structure of the related anion $[Cl_3W(\mu\text{-}SEt)(\mu\text{-}SEt_2)_2WCl_3]^-$ shows a slightly shorter W—W bond length [47] (Table 3). The W—S bond lengths are of interest in these structures. The thioether sulphur atoms are at slightly shorter distances than the thiolate sulphur atoms (2.37–2.39 Å for W—μ-S thioether; 2.43–2.84 Å for W—μ-S thiolate).

4. Methods of preparation

A number of general synthetic strategies now exist for synthesizing FBO complexes of Mo(III) and W(III). The simplest of these utilizes the dimerization of mononuclear M(III) precursors (Section 4.1) (e.g. MCl_3L_3, L≡phosphine). No analogous route exists for M(IV) or M(V) complexes. Reduction of M(IV) halides in the presence of appropriate ligands also leads to FBO M(III) complexes in many cases (Section 4.2). Metathesis reactions in which halide is replaced by a redox-active

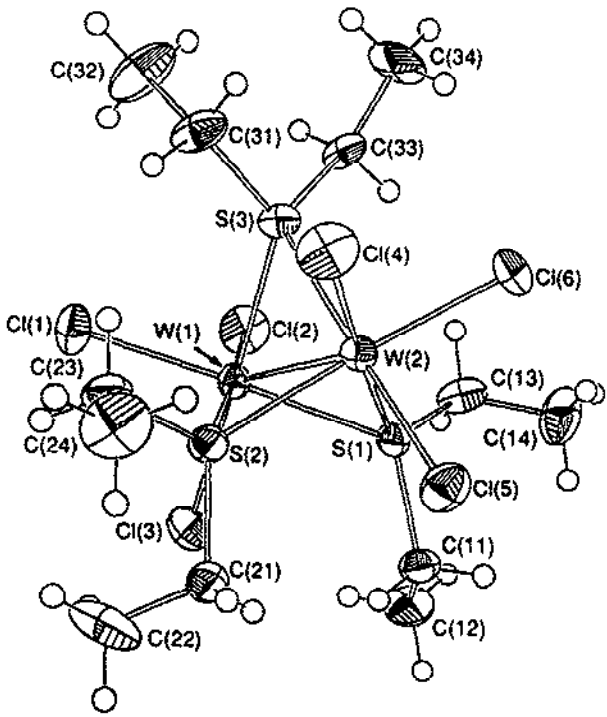

Fig. 14. ORTEP plot of the complex $[Cl_3W(\mu\text{-}SEt_2)_3WCl_3]$. (Reproduced with permission from Ref. [46].)

ligand have been used in certain instances to produce M(IV) FBO complexes and also mixed oxidation state M(IV)–M(III) species (Section 4.3). Strategies have also been developed for making certain mixed metal FBO complexes (Section 4.4). The higher oxidation state FBO complexes (especially M(V)) frequently arise as a result of the presence of oxo ligands in the coordination sphere. In many instances this has not been due to a planned synthesis but to the presence of adventitious oxygen in the reaction medium. In general it is probably fair to say that the synthesis of targeted FBO complexes from mononuclear precursors is rarely feasible other than in the area of M(III)–M(IV). The conversion of one FBO complex into another and the use of EBO complexes as precursors are alternative strategies which will be explored in Section 5.

4.1. Association of mononuclear precursors

Evidence for an equilibrium involving mononuclear $MoCl_3(THF)_3$ and an FBO complex was provided by Boyd and Wedd [62]. It was shown that $MoCl_3(THF)_3$ associates in CH_2Cl_2 to form the FBO complex $Mo_2Cl_6(THF)_3$, liberating three molecules of THF.

$$2MoCl_3(THF)_3 \rightleftharpoons Mo_2Cl_6(THF)_3 + 3THF$$

More recently Poli and Mui [63] have shown an equilibrium (see below) to exist for a variety of $MoX_3(THF)_3$ precursors (X≡Cl, Br). It was observed that the ^1H nuclear magnetic resonance (NMR) spectra of solutions of $MoX_3(THF)_3$ in CD_2Cl_2 change with time. In addition, the colour of the solutions darkens, becoming dark purple. Detailed paramagnetic NMR studies have shown that $Mo_2X_6(THF)_4$ is formed initially. In a subsequent step the edge-sharing complex $Mo_2X_6(THF)_4$ loses THF and the confacial complex $Mo_2X_6(THF)_3$ is formed.

$$2MoCl_3(THF)_3 \overset{\Delta,-2THF}{\rightleftharpoons} Mo_2Cl_6(THF)_4 \underset{+THF}{\overset{-THF}{\rightleftharpoons}} Mo_2Cl_6(THF)_3$$

Similar equilibria are thought of as being important for the $MoCl_3(MeCN)_3 \leftrightarrow Mo_2Cl_6(MeCN)_3$ interconversion [64]. $MoCl_3(THT)_3$ associates in toluene to give the antiferromagnetic $(THT)_2ClMo(\mu\text{-}Cl)_3MoCl_2(THT)$ and the diamagnetic $(THT)Cl_2Mo(\mu\text{-}Cl)_2(\mu\text{-}THT)MoCl_2(THT)$ [24]. Pure $(THT)Cl_2Mo(\mu\text{-}Cl)_2(\mu\text{-}THT)MoCl_2(THT)$ can be obtained by displacement of THF from $Mo_2Cl_6(THF)_3$ [24]. The labile ligands acetonitrile and THF are easily replaced in the presence of donors such as phosphines and thioethers. In fact, this reaction is a convenient route for the synthesis of FBO complexes. For example, the reaction of $MoX_3(THF)_3$ with phosphines leads to the formation of the FBO complexes *anti*-$L_2XMo(\mu\text{-}X)_3MoX_2L$(L≡$Et_3P$; X≡Cl [22]; L≡$Me_2PhP$; X≡Cl [22], Br, I [65]). In the presence of free halide anion $MoI_3(THF)_3$ reacts with phosphine to give the anion $[(Me_3P)I_2Mo(\mu\text{-}I)_3MoI_2(PMe_3)]$ [66].

An equilibrium between $MoCl_6^{3-}$ and $Mo_2Cl_9^{3-}$ and free chloride is thought not to involve the initial formation of the edge-sharing complex $Mo_2Cl_{10}^{4-}$ but to proceed directly to give the FBO nonachlorodimolybdate anion [67].

$$2MoCl_6^{3-} \rightleftharpoons Mo_2Cl_9^{3-} + 3Cl^-$$

4.2. Reduction of metal halides in the presence of ligand

In the absence of excess anionic ligands and the presence of neutral ligands the reduction of WCl_4 usually leads to the formation of FBO complexes possessing coordinated neutral ligands. As noted above, when thioethers are used as ligands in such reduction reactions, thioether-bridged systems are obtained possessing very short metal–metal bond distances. With other ligands, e.g. phosphines or ethers, FBO complexes containing terminally coordinated donors are formed. In the following, examples of such syntheses are given.

The reduction of WCl_4 by sodium amalgam in THF in the presence of PNP^+Cl^- leads to the formation of the PNP salt of the mixed oxidation state FBO anion $[W_2Cl_9]^{2-}$ [39]. An analogous reduction in the absence of free chloride yields the complex $[Na(THF)_3]^+[(THF)Cl_2W(\mu\text{-}Cl)_3WCl_2(THF)]^-$ [41]. This is a useful precursor for the d^3–d^3 ethane-like complexes $L_3M{\equiv}ML_3$, which were obtained upon reaction with LiX (X≡$CH_2{}^tBu$, NMe_2, O^{t}Bu) by Chisholm et al. [41].

The reduction of WCl_4 with Na/Hg in neat SEt_2 or THT leads to the formation

of the triply thioether-bridged complexes $Cl_3W(\mu\text{-}SR_2)_3WCl_3$ [46]. With SMe_2 the resulting complex is the anion $[Cl_3W(\mu\text{-}Cl)(\mu\text{-}SMe_2)_2WCl_3]^-$, which has been obtained before from the reaction of the hydride-bridged complex $[Cl_3W(\mu\text{-}H)(\mu\text{-}SMe_2)_2WCl_3]^-$ with benzyl chloride [45]. The reduction of $NbCl_5$ and $TaCl_5$ with Na/Hg in the presence of THT results in the formation of the M(III)–M(III) complexes $(THT)Cl_2M(\mu\text{-}Cl)_2(\mu\text{-}THT)MCl_2(THT)$ (M ≡ Nb, Ta), even in the presence of excess reducing agent [58,68]. However, further reduction of this complex is possible in THF to give the triply thioether-bridged Nb(II)–Nb(II) and Ta(II)–Ta(II) complexes $[Cl_3M(\mu\text{-}THT)_3MCl_3]^{2-}$ (M ≡ Nb, Ta) [69].

The reduction of WCl_4 in toluene in the presence of phosphines (PMe_2Ph, PBu_3), described by Cotton and Mandal [43], leads to the formation of complexes of the type $W_2Cl_6L_3$ containing terminal phosphines only. Interestingly, for the preparation of $W_2Br_6L_3$ (L ≡ PMe_2Ph, PMe_3), WBr_5 was used as a starting material.

The reduction of W(VI) complexes $WXCl_4$ (X ≡ NEt, NPh, O) with one equivalent of Na gives the binuclear tungsten(V) complexes $[W_2X_2Cl_7]^-$ [70]. All three complexes possess a μ-Cl bridge and terminal oxo or organoimido ligands.

$$2WXCl_4 + 2Na + R_4PCl \xrightarrow{CH_2Cl_2} (R_4P)[W_2X_2Cl_7] + 2NaCl$$

It is note worthy that the tungsten centres are in a strongly distorted octahedral environment due to the strong trans influence of the π donor, which causes the W–Cl bond trans to the W–X bond to be long.

4.3. Metathesis reactions

The reaction of $WCl_4(SMe_2)_2$ with R_3SiX (X ≡ H, D, SR, SeR) has been shown to result in the formation of confacial bioctahedral complexes [18,44,50,51,53]. A summary is given in Scheme 1.

Although plausible explanations for these products have been suggested, the syntheses cannot be classified as predictable routes to FBO complexes. It has been shown that the first step in the reaction between $WCl_4(SMe_2)_2$ and Me_3SiSR is the formation of labile $WCl_{4-n}(SR)_n(SMe_2)_2$ species, which then undergo degradation reactions to give the final products [50]. Depending on the stoichiometry of the reactants and the choice of silylthiolate, a variety of thiolate- and thiolate-sulphide-bridged complexes have been obtained. It is note worthy that in the reaction of $WCl_4(SMe_2)_2$ with Me_3Si–SePh a $(\mu\text{-}Se)(\mu\text{-}SePh)_2$-bridged complex is obtained [51], while in the analogous reaction with Me_3Si–SPh no S–C bond cleavage takes place and $[Cl_3W(\mu\text{-}Cl)(\mu\text{-}SPh)_2WCl_3]^{2-}$ is the exclusive product [53]. In the silylselenolate reaction a small amount of the paramagnetic μ-Cl species is formed, which is present within the lattice of the diamagnetic host complex $[Ph_4P][Cl_3W(\mu\text{-}Se)(\mu\text{-}SePh)_2WCl_3]$ [51].

In the presence of small traces of oxygen in the reaction mixture, invariably oxo complexes are formed, indicating the extreme oxophilicity of the tungsten species present in solution [55,56].

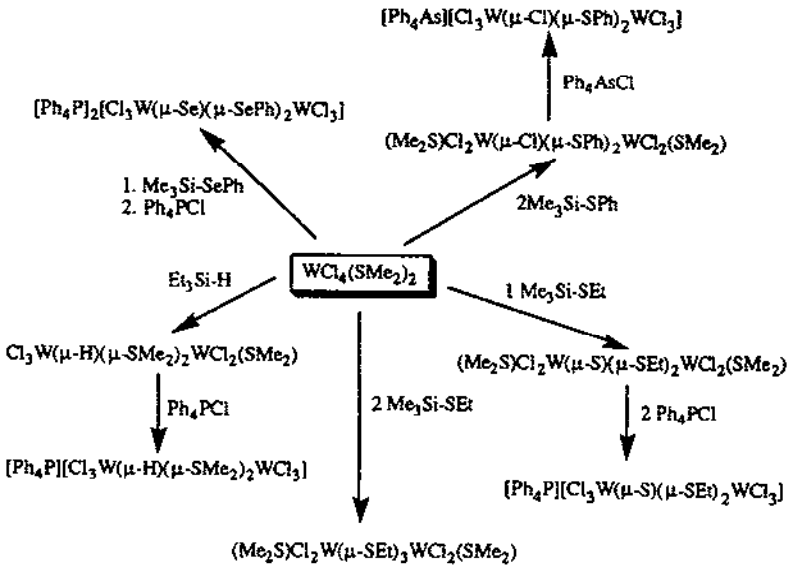

Scheme 1

The reaction of $WCl_4(SMe_2)_2$ with three equivalents of Et_3SiH in CH_2Cl_2 results in the formation of the hydride-bridged complex $Cl_3W(\mu\text{-}H)(\mu\text{-}SMe_2)_2WCl_2(SMe_2)$ [44]. The complex shows fluxional behaviour involving the exchange of the terminal and bridging thioether (see Section 5.2). The chloride derivative $[Ph_4P][Cl_3W(\mu\text{-}H)(\mu\text{-}SMe_2)_2WCl_3]$ has been crystallographically characterized. A similar reaction involving $MoCl_4(SMe_2)_2$ produces a mixture of compounds lacking the bridging hydrogen. Instead, the silane acts as a reducing reagent producing $(Me_2S)_2ClMo(\mu\text{-}Cl)_3MoCl_2(SMe_2)$ and $(Me_2S)Cl_2Mo(\mu\text{-}Cl)_2(\mu\text{-}SMe_2)MoCl_2(SMe_2)$ [23].

4.4. Miscellaneous

Other preparative routes to FBO complexes include solid state reactions such as that described by Broll et al. for the synthesis of octahalogendiniobate [57]. The oxidative displacement of carbon monoxide from $Mo(CO)_4Cl_3^-$ by $MoCl_6^{2-}$ leads to the formation of the nonachlorodimolybdate $Mo_2Cl_9^{3-}$ [71].

$$\left.\begin{array}{l} MCl_6^{2-} + Mo(CO)_4Cl_3^- \\ MoCl_6^{2-} + M(CO)_4Cl_3 \end{array}\right\rangle \rightarrow MMoCl_9^{3-}$$

It was thought that this route would provide an easy entry into the assembly of mixed metal FBO complexes. For the synthesis of the Cr—Mo FBO complex a similar approach was used. However, since neither $CrCl_6^{3-}$ nor $Cr(CO)_4Cl_3^-$ is available, a mixture of $CrCl_2$ and Cl^- is used as a synthon for $Cr(CO)_4Cl_3^-$. The reaction of $MoCl_6^{2-}$ with $\{CrCl_2, Cl^-\}$ proceeds cleanly to give the antiferromagnetic

$CrMoCl_9^{3-}$ [72]. Proof of the existence of $CrMoCl_9^{3-}$ was obtained from the UV–visible spectrum, which is distinctly different from that of a 1:1 mixture of $Cr_2Cl_9^{3-}$ and $Mo_2Cl_9^{3-}$.

The reactions of quadruply bonded M(II) complexes such as $[Mo_2(acetate)_4]$ with HCl or HBr were shown by Cotton and coworkers to yield the anions $[X_3Mo(Cl)_2(H)MoCl_3]^{3-}$ [26]. This was also the methodology adopted by Katovic and McCarley to produce the Mo—W analogues of the hydrido-bridged FBO anion as described in Table 2; they utilized the mixed acetate $MoW(acetate)_4$ in this synthesis [28]. Oxidation of $Mo_2I_4(PMe_3)_4$ with I_2 in toluene led to the synthesis of $[PHMe_3][Mo_2I_7(PMe_3)_2]$ [66]. Hence controlled oxidation of M(II) dimers has been successfully used as a route to a few FBO complexes.

$Mo(NNHPh)_2(butane\text{-}2,3\text{-}diolate)_2 \cdot H_2NNHPh$ reacts with excess thiophenol in methanol in the presence of Et_3N to give the complex $Mo_2(NNC_6H_5)_4(SC_6H_5)_5]^-$. This complex has a very long Mo Mo separation of 3.527(1) Å, indicating the absence of any metal–metal bonding [37].

The addition of a phenol to the ethane-like Mo_2 complex Mo(III)–Mo(III) dimer $(Me_2N)_3Mo{\equiv}Mo(NMe_2)_3$ in hexane results in the formation of the slightly paramagnetic complex (less than 0.3. μ_B by Evans' method) $(H_2NMe_2)[\{(Me_2N)(O\text{-}p\text{-}tol)_2Mo(\mu\text{-}O\text{—}ptol)_3Mo(O\text{—}p\text{-}tol)_2(NMe_2)\}]^-$ with a short Mo—Mo bond (2.60 Å). If more sterically hindered phenolate ligands are used, the product is not an FBO complex. It is thought that the deprotonation of coordinated phenol by free amine is involved in the formation of the FBO complex [33].

5. Reactivity studies

5.1. *Interconversion of edge- and face-sharing bioctahedral complexes*

As noted above, bioctahedral systems are obtained from mononuclear MX_3L_3 complexes (M ≡ Mo, W; X ≡ halide; L ≡ MeCN [64], THF [63,73] SR_2 [23,24]). In fact, this is the most widely used synthetic approach to FBO complexes. However, the yield of the FBO complex is often noticeably lower in the presence of excess ligand, suggesting competing reactions.

The first documented report of an equilibrium involving EBO-to-FBO transformation was provided in a short communication by Chacon et al. [42]. It was found that the FBO complex $(Me_3P)_2ClW(\mu\text{-}Cl)_3WCl_2(PMe_3)$ can be obtained from a solution of the EBO complex $W_2Cl_6(PEt_3)_4$ by removing all volatiles and recrystallization of the residue from CH_2Cl_2/Et_2O. A solution of the EBO complex $W_2Cl_6(PEt_3)_4$ in toluene-d_8 shows signals attributable to the corresponding FBO complex and free phosphine, indicating that an equilibrium exists according to

$$(Me_3P)_2Cl_2W(\mu\text{-}Cl)_2WCl_2(PMe_3)_2 \rightleftharpoons (Me_3P)_2ClW(\mu\text{-}Cl)_3WCl_2(PMe_3) + PMe_3$$

There is no spectral evidence for the existence of a mononuclear intermediate. However, in the case of molybdenum systems, mononuclear MoX_3L_3 species are

involved and are shown to play an integral part in the equilibrium between EBO and FBO.

Poli and Mui reported that the ^{1}H NMR spectra of solutions of $MoX_3(THF)_3$ in CD_2Cl_2 underwent significant changes; with time, signals appeared that could be attributed to the FBO complex $Mo_2X_6(THF)_3$ (*anti* and *gauche* isomers are present) and to the EBO complex $Mo_2X_6(THF)_4$ [63].

It was proposed that a series of equilibria exist:

$$2MoX_3(THF)_3 \rightleftharpoons Mo_2X_6(THF)_4 + 2THF$$

$$Mo_2X_6(THF)_4 \rightleftharpoons Mo_2X_6(THF)_3 + THF$$

In a first step $MoX_3(THF)_3$ condenses to give the edge-sharing complex $Mo_2X_6(THF)_4$ and free THF. The EBO complex then loses a molecule of THF to give the more stable FBO complex $Mo_2X_6(THF)_3$ and free THF. In the related phosphine systems the situation is much more complicated and the preferred species is strongly dependent on the amount of phosphine present in solution. In the presence of excess phosphine the mononuclear $MoX_3(PR_3)_3$ complex is the only stable species. ^{1}H NMR studies [22] on the Mo–phosphine systems reveal that the reaction of $MoCl_3(THF)_3$ with phosphines produces the EBO complex $Mo_2Cl_6(PR_3)_4$. This EBO complex is unstable with respect to the formation of the mononuclear $MoCl_3(PR_3)_3$ and the FBO complex $Mo_2Cl_6(PR_3)_3$ as per the following:

$$3Mo_2Cl_6L_4 \rightleftharpoons 2Mo_2Cl_6L_3 + 2MoCl_3L_3 \quad \text{for } L \equiv PEt_3,\ PMe_2Ph$$

The uptake of phosphine by the FBO complex to form the corresponding EBO complex is a fast process:

$$Mo_2Cl_6L_3 + L \rightarrow Mo_2Cl_6L_4 \quad \text{for } L \equiv PEt_3,\ PMe_2Ph$$

Scheme 2 [22], which is consistent with the ^{1}H NMR data, summarizes the relationship between mononuclear and binuclear EBO and FBO complexes.

The equilibrium between the EBO and FBO complexes is shifted significantly towards the EBO complex in the presence of phosphine. In a phosphine-rich environment the stability of Mo(III) complexes is $MoCl_3(PR_3)_3 \gg Mo_2Cl_6(PR_3)_4 > Mo_2Cl_6(PR_3)_3$.

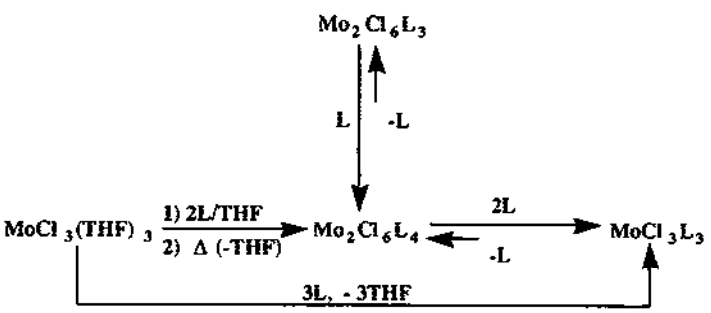

Scheme 2

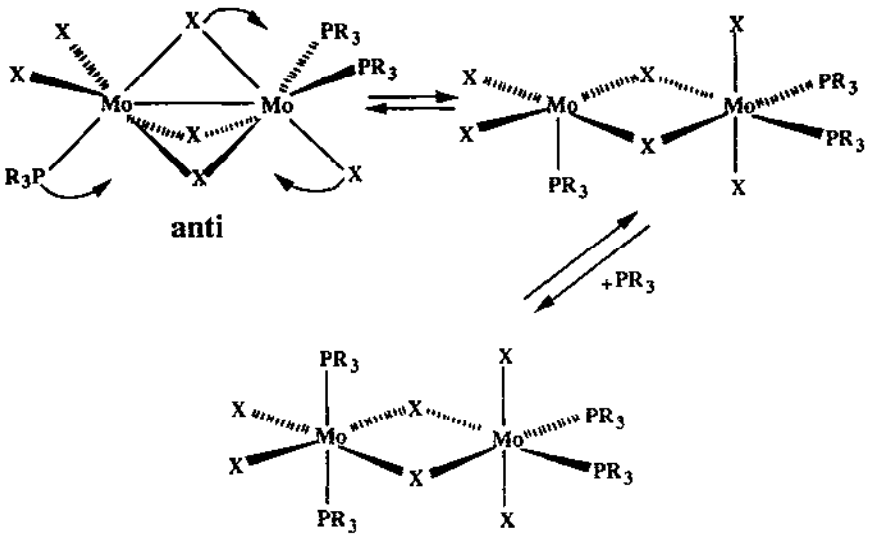

Fig. 15. Interconversion between EBO and FBO. (Adapted from Ref. [74].)

A possible mechanism for the interconversion between EBO and FBO complexes is shown in Fig. 15 [74].

The equilibrium reaction can only proceed from the *anti* FBO complex and not from the *gauche* FBO complex, since this would lead to an EBO complex of *eq*, *ax* coordination on one Mo centre with respect to the phosphines. Such a coordination has not been observed to date [5]. For the equilibrium between *anti* and *gauche* isomers, see below.

Canich and Cotton [75] have investigated the reactions of the FBO complexes $M_2Cl_6(SMe_2)_3$ (M ≡ Nb, Ta) with thioethers and phosphines (Fig. 16). They found

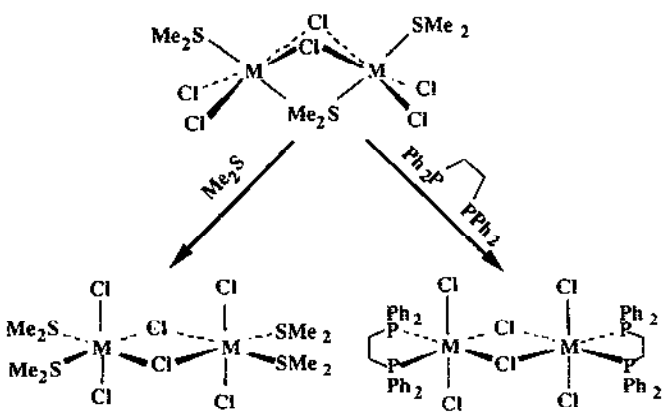

Fig. 16. Reaction of $M_2Cl_6(SMe_2)_3$ (M ≡ Nb, Ta) with thioethers and phosphines. (Adapted from Ref. [75].)

that upon reaction with excess thioether or phosphines, edge-sharing bioctahedral complexes are formed.

The authors suggested [75a] that an equilibrium exists between FBO and EBO complexes according to the following scheme. The addition of thioether will drive the equilibrium to the right, while removal will shift the equilibrium towards the FBO complex.

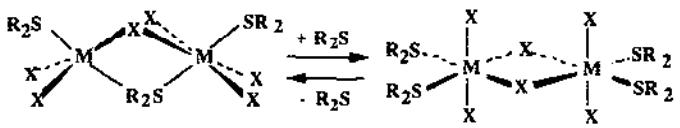

5.2. Ligand site exchange reactions

5.2.1. Bridging–terminal exchange

The first reported study of site exchange was made by Hawkins and Garner [76], who found in a radio-labelling experiment that all chlorides in $W_2Cl_9^{3-}$ are exchangeable for ^{36}Cl. Two possibilities for exchange were given but were not substantiated. It was postulated that either an intramolecular exchange or an equilibrium involving exchange intermediates might be responsible for interconversion of terminal and bridging chloride ligands.

A number of more recent studies have provided more insight into possible mechanisms. Boorman et al. [44] carried out a variable-temperature ^1H NMR study of the complex $[Cl_3W(\mu\text{-}H)(\mu\text{-}Me_2S)_2WCl_2(Me_2S)]$ in the range from -70 to $20\,^{\circ}C$. Two isomers could be identified at $-20\,^{\circ}C$, a C_s symmetry isomer (labelled meso) and an enantiomeric pair of C_1 isomers (labelled D, L pair). The ^1H resonances of the methyl groups of the Me_2S ligands provide a sensitive probe of the geometry and fluxional behaviour of these complexes. The structures of the isomers and the identity of the various CH_3 environments are shown in Fig. 17.

The *meso* isomer (C_s) is expected to give a ^1H NMR spectrum consisting of three singlets (intensity ratio 6:6:6) for the three inequivalent methyl groups (bridging thioether: axial and equatorial; terminal thioether) and a singlet due to the μ-hydride (intensity of unity).

For the two C_1 isomers one resonance for each methyl group would be expected at the low temperature limit. In the absence of inversion of the sulphur atom the two methyl groups on the terminal thioether will also be magnetically inequivalent. Hence for the C_1 isomers six resonances are expected in addition to a hydride signal.

The low temperature spectrum is consistent with the predictions made above. C_1 and *meso* isomers are present in a ratio of about 4:1. The amount of the *meso* isomers increases with time. Even a large excess of added SMe_2 does not alter the spectra, favouring an intramolecular process over an intermolecular process involving free thioether.

At least two fluxional processes must occur involving the pair of C_1 enantiomers. Inversion at the terminal thioether S causes the two resonances for the terminal SMe_2 protons in the C_1 isomers to collapse into a single resonance. The second

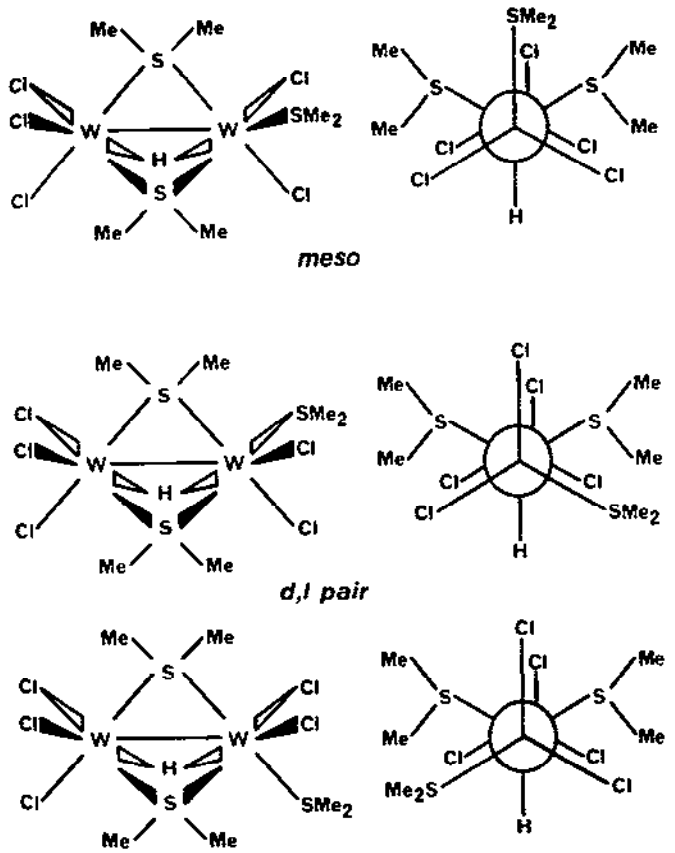

Fig. 17. Side views and end-on views of the possible geometric isomers for the complex $Cl_3W(\mu\text{-}H)(\mu\text{-}SMe_2)_2WCl_2(SMe_2)$ showing the possible environments of CH_3 groups. (Adapted from Ref. [44].)

process is a site exchange between the terminal thioether and the bridging thioether trans to it. At 20 °C only two methyl resonances occur for the C_1 enantiomers. One of these resonances corresponds to the two exchanging thioether ligands and is observed in a region between that typical for terminal and that for bridging thioethers. The second resonance is due to the thioether not involved in the exchange process. The exchange process renders the axial and equatorial sets of protons magnetically equivalent. Hence a resonance is observed at an average position between the axial and equatorial resonances for the pair of enantiomers. Fig. 18 shows the likely process which interconverts the two enantiomers leading to racemization.

As the first step in this racemization process, the longer $W-SMe_2$ bond trans to the terminal chloride has to break. After undergoing a Berry pseudorotation, the re-formation of a bond occurs between the five-coordinated tungsten and the thioether (formerly terminal).

The reaction of $Cl_3W(\mu\text{-}H)(\mu\text{-}SMe_2)_2WCl_2(SMe_2)$ with halide anion (Cl^- or Br^-) at 20 °C results in the substitution of the labile terminal thioether and the formation

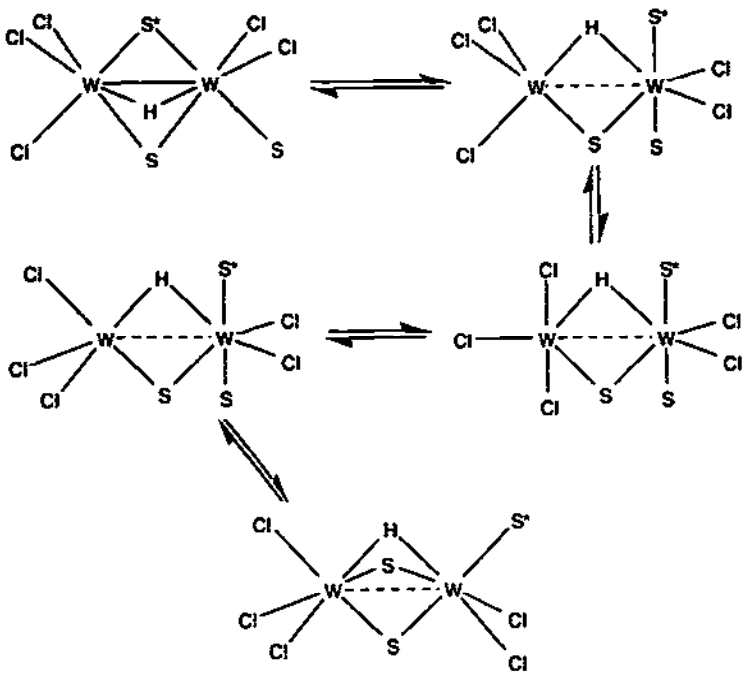

Fig. 18. Exchange of bridging and terminal thioether in $(Me_2S)Cl_2W(\mu\text{-}H)(\mu\text{-}SMe_2)_2WCl_3$ (S, S* ≡ SMe_2). (Adapted from Ref. [44].)

of $[Cl_3W(\mu\text{-}H)(\mu\text{-}SMe_2)WCl_2X]^-$. In the case of Br^- the ^1H NMR signals of the (μ-Me_2S) ligands show that the stereochemistry is retained and no exchange with bridging ligands occurs at ambient temperature.

It is interesting to note that Cotton and Poli's anion $[(Me_3P)I_2Mo(\mu\text{-}I)_3MoI_2(PMe_3)]^-$ does not undergo halide exchange with free chloride anion. Reaction in acetone/methanol with Ph_4AsCl results in a cation exchange only [31].

An interesting isomerization occurs between a terminal and a bridging thioether in d^3–d^3 Mo FBO complexes. It was noted that the complex C_s *anti*-$[(R_2S)_2ClMo(\mu\text{-}Cl)_3MoCl_2(SR_2)]$ is unstable towards the formation of the diamagnetic, C_{2v} symmetry, thioether-bridged complex $(R_2S)Cl_2Mo(\mu\text{-}SR_2)(\mu\text{-}Cl)_2MoCl_2(SR_2)$ [23]. The presence of a bridging thioether causes the two metals to be in close contact (d(Mo—Mo) = 2.462 Å for SMe_2 and d(Mo—Mo) = 2.470 Å for $SR_2 \equiv$ THT). Accompanying the shortening of the Mo—Mo distance is a change in spin states from antiferromagnetic (Bleaney–Bowers treatment indicates a triplet spin state, $J_{obs} = -420\,cm^{-1}$) behaviour to diamagnetic behaviour for $(R_2S)Cl_2Mo(\mu\text{-}SR_2)(\mu\text{-}Cl)_2MoCl_2(SR_2)$. It was noted that the process was not affected by the presence of free thioether, suggesting an internal process similar to the one described above.

MO calculations based on density functional theory show that the $(R_2S)Cl_2Mo(\mu$-

$SR_2)(\mu\text{-}Cl)_2MoCl_2(SR_2)$ is more stable than the antiferromagnetic *anti*-$(R_2S)_2ClMo(\mu\text{-}Cl)_3MoCl_2(SR_2)$ isomer in terms of total bonding energy by 11.6 kJ mol^{-1}. The calculated Mo—(μ-SR_2)—Mo bond strength (−135 kJ mol^{-1}) is 52.3 kJ mol^{-1} higher than the terminal Mo—SR_2 bond strength [60], thus providing a thermodynamic rationale for this isomerization process.

5.2.2. Interconversion of syn and gauche isomers

The solid state structure of the $[(Me_3P)I_2Mo(\mu\text{-}I)_3MoI_2(PMe_3)]$ anion [31] shows the two terminal phosphine ligands to be in the *syn* configuration. However, in acetone-d_6 solution the interconversion between *syn* and *gauche* isomers was observed to a final equilibrium concentration of 1:2. The free energy of activation for this process was determined to be 21.4 kcal mol^{-1} (for *syn* to *gauche*; 21.8 kcal mol^{-1} for *gauche* to *syn*). Owing to the substitutional inertness of Mo(III) systems, an intramolecular rearrangement was assumed, not unlike the one described for the interconversion of bridging and terminal thioethers in $Cl_3W(\mu\text{-}H)(\mu\text{-}SMe_2)_2WCl_2(SMe_2)$ [44]. For the chloride analogue a similar isomerization process was observed. However, the addition of PMe_3 slows down this process, indicating a dissociative pathway for the isomerization process [29]. In fact, both isomers could be obtained as crystalline solids, allowing direct structural comparisons to be made.

In the solid state, $Mo_2X_6L_3$ systems (L ≡ monodentate phosphine) have been shown to exist as the anti isomer exclusively. However, ^1H NMR studies of solutions show that both the *gauche* and *anti* isomers are present [21,22,65] (Fig. 19).

Upon dissolution of *anti*-$(Me_3P)_2Mo(\mu\text{-}Cl)_3MoCl_2(PMe_3)$ in $CDCl_3$ or acetone-d_6 two peaks are present in the ^1H NMR spectrum in a 2:1 ratio, indicating a facile process interconverting the two isomeric forms [74]. Assuming faster substitution in the position trans to the phosphine as compared with the chloride, Fig. 20 shows a plausible mechanism as described by Poli and Gordon [74]. Any of the Mo—(μ-Cl)—Mo bonds, all being trans to a phosphine, can be broken and, invoking the principle of microscopic reversibility, re-formed. A route via EBO complexes does not have to be invoked.

5.3. Ligand displacement reactions

5.3.1. Breakdown of the FBO framework

As early as 1956, Jonassen et al. [77] reported the isolation of $W_2Cl_6(py)_3$ from the reaction of $W_2Cl_9^{3-}$ with pyridine. It was believed that the bridging region

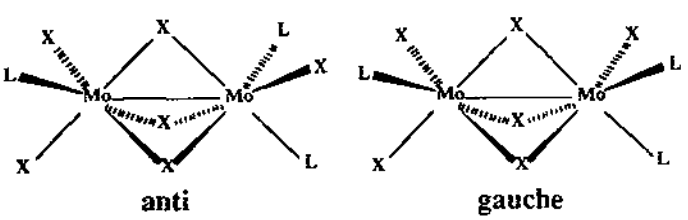

Fig. 19. *Anti* and *gauche* isomers of $Mo_2X_6L_3$ systems.

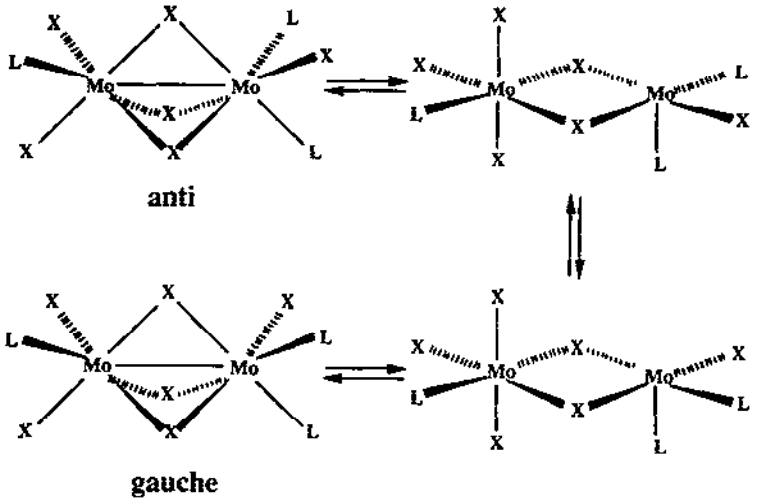

Fig. 20. Possible mechanism for the interconversion of *anti* and *gauche* isomers of $(R_3P)Cl_2Mo(\mu\text{-}Cl)_3MoCl(PR_3)_2$. (Adapted from Ref. [74].)

remains unchanged and that substitution of the terminal chloride ligands takes place instead. Later studies of the reaction of the easily accessible FBO complex $K_3W_2Cl_9$ with the nitrogen bases pyridine, 4-picoline and 4-isopropyl pyridine concluded that the products are actually the diamagnetic complexes $W_2Cl_6(py)_4$ [78]. Determination of the structure by X-ray crystallography confirmed $W_2Cl_6(py)_4$ to possess an edge-sharing bioctahedral arrangement [79].

The reactions of $[Cl_3W(\mu\text{-}H)(\mu\text{-}SMe_2)_2WCl_2(SMe_2)]$ and the anion $[Cl_3W(\mu\text{-}H)(\mu\text{-}SMe_2)_2WCl_3]^-$ with pyridine result in the formation of the EBO complex $(py)_2Cl_2W(\mu\text{-}Cl)(\mu\text{-}H)WCl_2(py)_2$. The bridging hydride is retained in this complex [45]. Analogous compounds were made by Carlin and McCarley by reaction of $W_2(mhp)_4$ (mhp ≡ anion of 6-methyl-2-hydroxypyridine) with Me_3SiCl and various substituted pyridines. The structure of $W_2HCl_5(NC_5H_4C_2H_5)_4$ was determined [80]. In contrast with this result, the analogous reactions of $Mo_2X_9^{3-}$ and the related $Mo_2X_8H^{3-}$ (with X ≡ Cl, Br) with pyridine lead to the complete degradation of the FBO framework to give mononuclear *mer*-$MoCl_3(py)_3$ in high yields [81]. The incomplete reaction of $Mo_2X_8H^{3-}$ with pyridine allows the isolation of the binuclear complex $Mo_2X_4(py)_4$. Since $Mo_2X_4(pg)_4$ reacts with pyridine to form *mer*-$MoCl_3(py)_3$, it is believed that the Mo(II) binuclear complex is an intermediate in the formation of *mer*-$MoCl_3(py)_3$ from $Mo_2X_8H^{3-}$ [81].

5.3.2. Retention of the FBO framework

The electrolysis of a solution of $Cs_3Mo_2Cl_8H$ in aqueous HBr leads to the replacement of the bridging hydride ligand by bromide and the formation of $Cs_3Mo_2Br_9$ [81]. The replacement of the μ-hydride is also observed by reacting $Cs_3Mo_2Br_8H$ with aqueous HBr. The reaction proceeds with hydrogen evolution and the formation of the all-bromo anion $W_2Br_9^{3-}$ [82].

The bridging hydride of $[Cl_3W(\mu\text{-}H)(\mu\text{-}SMe_2)_2WCl_2(SMe_2)]$ and $(Ph_4P)[Cl_3W(\mu\text{-}H)(\mu\text{-}SMe_2)_2WCl_3]$ reacts with benzyl chloride at elevated temperatures to give the chloro-bridged complex $[Cl_3W(\mu\text{-}Cl)(\mu\text{-}SMe_2)_2WCl_3]^-$. Toluene was identified as the organic byproduct of this reaction [45]. It is note worthy that in the case of the neutral compound $[Cl_3W(\mu\text{-}H)(\mu\text{-}SMe_2)_2WCl_2(SMe_2)]$, benzyl chloride alkylates sulphur of the terminal thioether to form the sulphonium cation $[PhCH_2(CH_2)_2S]^+$. The alkylation of the thioether after dissociation has to be considered as a possible route to the sulphonium cation. It is important to point out that the bridging thioether is not alkylated, presumably because of the involvement of its lone pairs in donation to the two metal centres, which will undoubtedly reduce the nucleophilic character of the bridging thioether [45]. A similar reaction for the neutral complex and its derived anion has been observed with benzyl bromide [83].

$$[Cl_3W(\mu\text{-}H)(\mu\text{-}SMe_2)_2WCl_3]^- + RX \rightarrow [Cl_3W(\mu\text{-}X)(\mu\text{-}SMe_2)WCl_3]^- + RH$$

$$[Cl_3W(\mu\text{-}H)(\mu\text{-}SMe_2)_2WCl_2(SMe_2)] + 2RX \rightarrow$$

$$[RMe_2S]^+[Cl_3W(\mu\text{-}X)(\mu\text{-}SMe_2)WCl_2X]^- + RH$$

Terminal ligands are often substitutionally labile and can be easily replaced by stronger donors. A good example is the reaction of $(THF)_2ClMo(\mu\text{-}Cl)_3MoCl_2(THF)$ with PMe_3 [74]. All terminal THF molecules are replaced to give the trisphosphine complex $(Me_3P)_2ClMo(\mu\text{-}Cl)_3MoCl_2(PMe_3)$. Its reaction with PPNCl results in the replacement of one of the phosphines to give the corresponding anion $[(Me_3P)Cl_2Mo(\mu\text{-}Cl)_3MoCl_2(PMe_3)]^-$.

$$Mo_2Cl_6(THF)_3 + 2PMe_3 + PPN^+Cl^- \rightarrow (PPN)[Mo_2Cl_7(PMe_3)_2]$$

The anion was obtained earlier by the oxidative addition of Cl_2 to $Mo_2Cl_4(PMe_3)_4$ as an $HPMe_3^-$ salt by Cotton and Luck [29]. Its structure is similar to that reported by Cotton and Poli for the analogous iodo complex $[Mo_2I_7(PMe_3)_2]^-$ [31].

5.4. *Reactions of coordinated ligands*

Some unexpected reactivity for FBO complexes has recently been reported by Boorman et al. [47,48]. The reactions of anionic nucleophiles with the triply thioether-bridged systems $Cl_3W(\mu\text{-}SR_2)_3WCl_3$ were studied, with the anticipation of replacement of the terminal chlorides or a conversion to EBO structures [47]. However, the reaction is thioether based and nucleophilic attack at the thioether results in S—C bond cleavage, leading to the formation of a $[Cl_3W(\mu\text{-}SR)(\mu\text{-}SR_2)_2WCl_3]^-$ anion (Fig. 21).

The reaction of $Cl_3W(\mu\text{-}SEt_2)_3WCl_3$ with a variety of nucleophiles leads to S—C bond cleavage and the quantitative formation of a μ-ethylthiolate binuclear anion. In addition, the expected organic byproducts can be isolated quantitatively. If the μ-THT analogue is subjected to similar reactions, the nucleophilic attack leads to the formation of a μ-butanethiolato FBO anion, with the nucleophile remaining attached to the aliphatic chain. The crystal structure of the binuclear anion $[Cl_3W(\mu\text{-}$

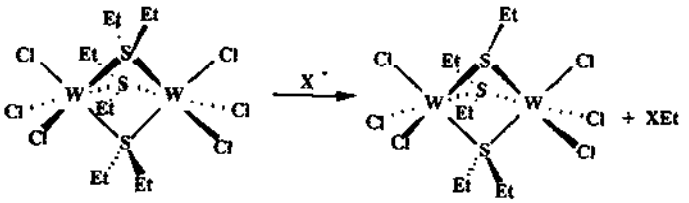

Fig. 21. Reaction of $Cl_3W(\mu\text{-}SEt_2)_3WCl_3$ with anionic nucleophiles. (Adapted from Ref. [47].)

$S(CH_2)_4Cl)(\mu\text{-}THT)_2WCl_3]^-$ was determined by an X-ray diffraction study and shows that the FBO framework remains unaltered [47] (Fig. 22).

When $\{Ph_4P\}[Cl_3W(\mu\text{-}Cl)(\mu\text{-}SR_2)_2WCl_3]$ was allowed to react with nucleophiles such as thiolate, S−C bond cleavage took place, leading to the formation of an FBO dianion with three different bridging ligands, $\{Ph_4P\}_2[Cl_3W(\mu\text{-}Cl)(\mu\text{-}SR)(\mu\text{-}SR_2)WCl_3]$ (R ≡ Me, Et). Its crystal structure is shown in Fig. 23 and allows the direct comparison of W−(μ-Cl), W−(μ-SR_2) and W−(μ-SR) bond lengths within the same complex (see Section 3) [48].

These reactions, in which the C−S bond of a μ-thioether is cleaved by a nucleo-

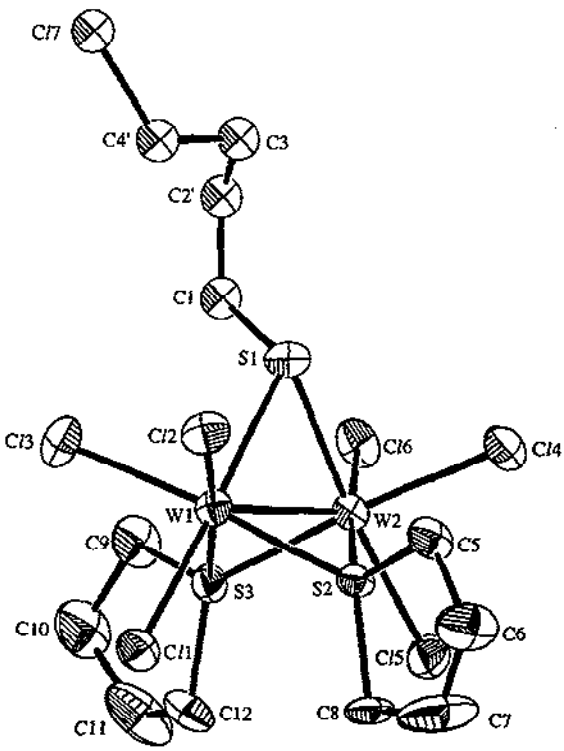

Fig. 22. ORTEP plot of the anion $[Cl_3W(\mu\text{-}S(CH_2)_4Cl)(\mu\text{-}THT)_2WCl_3]^-$. (Reproduced with permission from Ref. [47].)

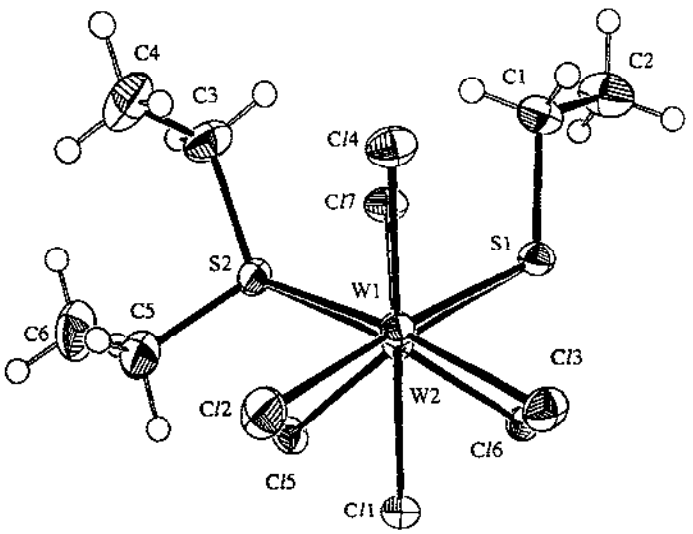

Fig. 23. ORTEP plot of the anion $[Cl_3W(\mu\text{-}Cl)(\mu\text{-}SEt)(\mu\text{-}SEt_2)WCl_3]$ as viewed along the W—W vector. (Reproduced with permission from Ref. [48].)

phile, are notable for at least two reasons. First, the MO calculations [60] showed that for d^3–d^3 systems there would be back donation of electron density into a σ^* orbital associated with the C—S bonds, thereby causing a weakening of these bonds (see Fig. 13). The second point of interest lies in the fact that one of the nucleophiles used in this study was hydride:

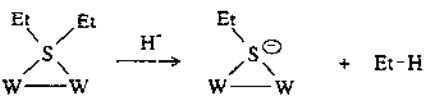

The reaction therefore represents an analogue of the industrially important hydrodesulphurization (HDS) process. Thus the study of these relatively simple binuclear species may provide a model for surface reactions on metal sulphide catalysts [84].

5.5. *Oxidative addition reactions*

The only oxidative addition chemistry of FBO complexes so far reported has been done on Group 5 complexes and this has been reviewed by Messerle [85]. However, one example will be given because of its relevance to the S—C bond activation chemistry exhibited by its tungsten analogue. The attempted reduction of $Ta_2Cl_6(SMe_2)_3$ with sodium amalgam in the presence of two equivalents of $^tPr_2P(CH_2)_3P^iPr_2$ (dippp) under an atmosphere of dihydrogen (4 atm) led to the formation of black crystals (in 70% yield), which were identified by X-ray crystallography and ^1H NMR as the ditantalum(IV) complexes [(dippp)HClTa(μ-S)(μ-H)$_2$TaHCl(dippp)] [86]. Cleavage of the S—C bond is involved, leading to a μ-sulphido ligand, and one might speculate that at least one

of the steps leading to the formation of this complex is the nucleophilic attack of the coordinated SMe_2 by a hydride ligand. If the reaction mechanism were the same as that of the tungsten complexes $Cl_3W(\mu\text{-}SR_2)_3WCl_3$ and $[Cl_3W(\mu\text{-}Cl)(\mu\text{-}SR_2)_2WCl_3]^-$, methane would be the expected byproduct of the reaction. However, methane was not observed; instead, ethane was produced (gas chromatography–mass spectrometry). When the related complex $Ta_2Cl_6(THT)_3$ was subjected to the same reaction conditions, the edge-sharing bioctahedral complex $[(dippp)H_2Ta(\mu\text{-}H)_2TaH_2(dippp)]$ was isolated and identified by NMR spectroscopy [86].

5.6. *Redox chemistry*

The one-electron oxidation of $W_2Cl_9^{3-}$ with halogens [87] (Cl_2, Br_2 and I_2) leads to the formation of the mixed valence anion $W_2Cl_9^{2-}$:

$$2W_2Cl_9^{3-} + X_2 \rightarrow 2W_2Cl_9^{2-} + 2X^-$$

Cotton et al. [39] have also produced this anion by reduction of WCl_4 with Na/Hg in the presence of PPNCl in THF. Crystallographic determination of the structure of $W_2Cl_9^{2-}$ allowed structural comparisons to be made between $W_2Cl_9^{3-}$ and $W_2Cl_9^{2-}$. As expected (Section 3), the removal of an electron from $W_2Cl_9^{3-}$ leads to a small but significant increase in the W—W bond length.

6. Conclusions

The synthesis of specific targeted examples of FBO complexes of molybdenum or tungsten is still rarely possible except for certain well-established M(III)–M(III) systems. For this particular class there is now a significant body of data relating to the dimerization of mononuclear MX_3L_3 complexes to yield FBO $M_2L_6L_3$ systems. However, the preparation of FBO complexes of M(IV) and M(V) has been largely a matter of serendipity. Oxo ligands are frequently found in such species, often not planned by the authors. The inherently weaker metal–metal interactions present for these more electron-poor species is doubtless a major determinant of this observation.

The detailed structural features of many FBO complexes have been explained by MO calculations based on the fragment approach. Furthermore, such calculations have often led to a rationalization of their reactivity patterns. Again, the most well-understood and predictable chemistry is that of the M(III)–M(III) FBO complexes. This would be anticipated on the basis of these d^3–d^3 systems having optimal electronic configurations for metal–metal bonding interactions. This is particularly pronounced in the case of ditungsten complexes.

The reaction patterns for FBO complexes have so far been quite limited in scope in comparison with mononuclear octahedral complexes. However, there are some signs that there is still much to discover. The interconversion between FBO $M_2L_6L_3$ and EBO $M_2L_6L_4$ complexes, the exchange between terminal and bridging ligands and the reactivity of bridging ligands in FBO complexes all support this prognosis. The exploration of potential catalytic activity of selected FBO complexes has com-

menced in the authors' laboratory. This was prompted by the publication of a series of papers by Cotton et al. [7] on the reactivity of $Nb_2Cl_6(thioether)_3$ systems towards alkynes and the general interest in cooperativity between metals in the activation of small molecules. The preliminary results of our research [88] suggest that both the C_{2v} and C_s isomers of $Mo_2Cl_6(thioether)_3$ will catalyse the polymerization and/or cyclotrimerization of selected alkynes. The possibility that the active catalytic species is actually a mononuclear species cannot be rejected at this point. The inactivity of tungsten FBO complexes, with their inherently stronger W—W interactions, would tend to support this interpretation, but the structures of the $M_2Cl_6L_3$ ($M \equiv Mo, W$) complexes are not the same (see Section 3) and hence comparisons are not strictly valid. Even if they do turn out to be merely catalyst precursors, the potential for expansion of the field of catalytic properties of FBO complexes of molybdenum has at least been established.

The coupling of FBO complexes themselves, to yield chains of ligand-bridged dimers, is an attractive target in the present climate of interest in new materials. Such an approach might afford pathways to extended structures under relatively mild conditions. Most of the attention so far seems to have been paid to the reactions of unsupported (i.e. no bridging ligands) metal–metal-bonded M(III)–M(III) complexes. FBO complexes perhaps deserve greater popularity as research targets.

Acknowledgement

We thank the Natural Sciences and Engineering Research Council of Canada for financial support.

References

[1] F.A. Cotton and R.A. Walton, Multiple Bonds between Metal Atoms, Wiley, New York, 1982.
[2] F.A. Cotton, Acc. Chem. Res., 11 (1978) 225.
[3] F.A. Cotton, Polyhedron, 5 (1986) 3.
[4] F.A. Cotton and R.A. Walton, Struct. Bond. (Berlin), 62 (1985) 1.
[5] F.A. Cotton, Polyhedron, 6 (1987) 667.
[6] P.E. Kazin, V.I. Spitsyn and V.V. Zelentsov, Russ. Chem. Rev., 58 (1989) 1157.
[7] F.A. Cotton, W.T. Hall, K.J. Cann and F.J. Karol, Macromolecules, 14 (1981) 233.
[8] F.A. Cotton and D.A. Ucko, Inorg. Chim. Acta, 6 (1972) 161.
[9] R. Stranger, P.W. Smith and I.E. Grey, Inorg. Chem., 28 (1989) 1271.
[10] L. Dubicki, E. Krausz, R. Stranger, P.W. Smith and Y. Tanabe, Inorg. Chem., 26 (1987) 2247.
[11] (a) R. Stranger, Chem. Phys. Lett., 157 (1989) 472.
(b) R. Stranger, Inorg. Chem., 29 (1990) 5231.
[12] D.V. Korol'kov and K. Missner, Teor. Eksp. Khim., 9 (1973) 336.
[13] L. Natkanice, Bull. Pol. Acad. Sci. Chem., 26 (1978) 633.
[14] A.P. Ginsberg, J. Am. Chem. Soc., 102 (1980) 111.
[15] R.H. Summerville and R. Hoffmann, J. Am. Chem. Soc., 101 (1979) 3821.
[16] W.C. Trogler, Inorg. Chem., 19 (1980) 697.
[17] J.L. Templeton, R.A. Jacobsen and R.E. McCarley, Inorg. Chem., 16 (1977) 3320.
[18] P.M. Boorman, V.D. Patel, K.A. Kerr, P.W. Codding and P. van Roey, Inorg. Chem., 19 (1980) 3508.

[19] J.L. Templeton, W.C. Dorman, J.C. Clardy and R.E. McCarley, Inorg. Chem., 17 (1978) 1263.
[20] A. Bino, B.E. Bursten, F.A. Cotton and A. Fang, Inorg. Chem., 21 (1982) 3755.
[21] F.A. Cotton, R.L. Luck and K.-A. Son, Inorg. Chim. Acta, 173 (1990) 131.
[22] R. Poli and H.D. Mui, Inorg. Chem., 30 (1991) 65.
[23] P.M. Boorman, K.J. Moynihan and R.T. Oakley, J. Chem. Soc., Chem. Commun., (1982) 899.
[24] K.J. Moynihan, X. Gao, P.M. Boorman, J.F. Fait, G.K.W. Freeman, P. Thornton and D.J. Ironmonger, Inorg. Chem., 29 (1990) 1648.
[25] R. Saillant, R.B. Jackson, W.E. Streib, K. Folting and R.A.D. Wentworth, Inorg. Chem., 10 (1971) 1453.
[26] (a) M.J. Bennett, J.V. Brencic and F.A. Cotton, Inorg. Chem., 8 (1969) 1060.
(b) F.A. Cotton, B.A. Frenz and Z.C. Mester, Acta Crystallogr. B, 29 (1973) 1515.
(c) F.A. Cotton and B.J. Kalbacher, Inorg. Chem., 15 (1976) 522.
[27] A. Bino and F.A. Cotton, Angew. Chem., Int. Edn. Engl., 18 (1979) 332.
[28] (a) V. Katovic and R.E. McCarley, J. Am. Chem. Soc., 100 (1978) 5586.
(b) V. Katovic and R.E. McCarley, Inorg. Chem., 17 (1978) 1268.
[29] F.A. Cotton and R.L. Luck, Inorg. Chem., 28 (1989) 182.
[30] R.C. Gordon, H.D. Mui and R. Poli, Polyhedron, 10 (1991) 1667.
[31] F.A. Cotton and R. Poli, Inorg. Chem., 26 (1987) 3310.
[32] M.H. Chisholm, J. Organomet. Chem., 239 (1982) 79.
[33] T.W. Coffindaffer, I.P. Rothwell and J.C. Huffman, Inorg. Chem., 22 (1983) 3179.
[34] P.T. Bishop, J.R. Dilworth, J. Hutchinson and J.A. Zubieta, J. Chem. Soc., Chem. Commun., (1982) 1052.
[35] I.W. Boyd, I.G. Dance, A.E. Landers and A.G. Wedd, Inorg. Chem., 18 (1979) 1875.
[36] G. Bunzey, J.H. Enemark, J.I. Gelder, K. Yamanouchi and W.E. Newton, J. Less-Common Met., 54 (1977) 101.
[37] T.-C. Hsieh and J. Zubieta, Inorg. Chim. Acta, 99 (1985) L47.
[38] W.H. Watson and J. Waser, Acta Crystallogr., 11 (1958) 689.
[39] F.A. Cotton, L.R. Falvello, G.N. Mott, R.R. Schrock and L.G. Sturgeoff, Inorg. Chem., 22 (1983) 2621.
[40] D.J. Bergs, M.H. Chisholm, K. Folting, J.C. Huffman and K. Stahl, Inorg. Chem., 27 (1988) 2950.
[41] M.H. Chisholm, B.W. Eichhorn, K. Folting, J.C. Huffman, C.D. Ontiveros, W.E. Streib and W.G. Van Der Sluys, Inorg. Chem., 26 (1987) 3182.
[42] S.T. Chacon, M.H. Chisholm, W.E. Streib and W. Van Der Sluys, Inorg. Chem., 28 (1989) 6.
[43] F.A. Cotton and S.K. Mandal, Inorg. Chem., 31 (1992) 1267.
[44] P.M. Boorman, K.J. Moynihan, V.D. Patel and J.F. Richardson, Inorg. Chem., 24 (1985) 2989.
[45] P.M. Boorman, K.J. Moynihan and J.F. Richardson, Inorg. Chem., 27 (1988) 3207.
[46] P.M. Boorman, X. Gao, G.K.W. Freeman and J.F. Fait, J. Chem. Soc., Dalton Trans., (1991) 115.
[47] P.M. Boorman, X. Gao, J.F. Fait and M. Parvez, Inorg. Chem., 30 (1991) 3886.
[48] P.M. Boorman, X. Gao and M. Parvez, J. Chem. Soc., Dalton Trans., (1992) 25.
[49] J.T. Barry, S.T. Chacon, M.H. Chisholm, V.F. DiStasi, J.C. Huffman, W.E. Streib and W.G. Van Der Sluys, Inorg. Chem., 32 (1993) 2322.
[50] J.M. Ball, P.M. Boorman, K.J. Moynihan, V.D. Patel, J.F. Richardson, D. Collison and F.E. Mabbs, J. Chem. Soc., Dalton Trans., (1983) 2479.
[51] J.M. Ball, P.M. Boorman, J.F. Fait, H.-B. Kraatz, J.F. Richardson, D. Collison and F.E. Mabbs, Inorg. Chem., 29 (1990) 3290.
[52] S.T. Chacon, M.H. Chisholm, K. Folting, M.J. Hampden-Smith and J.C. Huffman, Inorg. Chem., 30 (1990) 3122.
[53] P.M. Boorman, P.W. Codding, K.A. Kerr, K.J. Moynihan and V.D. Patel, Can. J. Chem., 60 (1982) 1333.
[54] M.H. Chisholm, E.A. Lucas, A.C. Sousa, J.C. Huffman, K. Folting, E.B. Lobkovsky and W.E. Streib, J. Chem. Soc., Chem. Commun., (1991) 847.
[55] V.D. Patel, P.M. Boorman, K.A. Kerr and K.J. Moynihan, Inorg. Chem., 21 (1982) 1383.
[56] J.M. Ball, P.M. Boorman, K.J. Moynihan and J.F. Richardson, Acta Crystallogr C, 41 (1985) 47.
[57] A. Broll, H.G. von Schnering and H. Schaefer, J. Less-Common Met., 22 (1970) 243.

[58] E.T. Maas Jr. and R.E. McCarley, Inorg. Chem., 12 (1973) 1096.
[59] F.A. Cotton, S.A. Duraj and W.J. Roth, Acta Crystallogr., C, 41 (1985) 878.
[60] H. Jacobsen, H.-B. Kraatz, T. Ziegler and P.M. Boorman, J. Am. Chem. Soc., 114 (1993) 7851.
[61] F.A. Cotton, M.P. Diebold and W.J. Roth, J. Am. Chem. Soc., 108 (1986) 3538.
[62] I.W. Boyd and A.G. Wedd, Aust. J. Chem., 29 (1976) 1829.
[63] R. Poli and H.D. Mui, J. Am. Chem. Soc., 112 (1990) 2446.
[64] C. Miniscloux, G. Martino and L. Sajus, Bull. Soc. Chim. Fr., (1973) 2179.
[65] J.C. Gordon, H.D. Mui, R. Poli and K.J. Ahmed, Polyhedron, 10 (1991) 1667.
[66] F.A. Cotton and R. Poli, Inorg. Chem., 26 (1987) 3310.
[67] P.W. Smith and A.G. Wedd, J. Chem. Soc. A, (1970) 2447.
[68] F.A. Cotton and R.C. Nijjar, Inorg. Chem., 20 (1981) 2716.
[69] F.A. Cotton, M.P. Diebold and W.J. Roth, J. Am. Chem. Soc., 109 (1987) 5506.
[70] D.C. Bradley, R.J. Errington, M.B. Hursthouse and R.L. Short, J. Chem. Soc., Dalton Trans., (1990) 1043.
[71] W.H. Delphin and R.A.D. Wentworth, J. Am. Chem. Soc., 95 (1973) 7920.
[72] M.S. Matson and R.A.D. Wentworth, J. Am. Chem. Soc., 93 (1975) 7838.
[73] M.W. Anker, J. Chatt, G.J. Leigh and A.G. Wedd, J. Chem. Soc., Dalton Trans., (1975) 2639.
[74] R. Poli and J.C. Gordon, J. Am. Chem. Soc., 114 (1992) 6723.
[75] (a) J.A.M. Canich and F.A. Cotton, Inorg. Chem., 26 (1987) 3473.
(b) J.A.M. Canich and F.A. Cotton, Inorg. Chem., 26 (1987) 4236.
[76] G.L. Hawkins and C.S. Garner, J. Am. Chem. Soc., 80 (1958) 2946.
[77] H.B. Jonassen, S. Cantor and A.R. Tarsey, J. Am. Chem. Soc., 78 (1956) 271.
[78] R. Saillant, J.L. Hayden and R.D.A. Wentworth, Inorg. Chem., 6 (1967) 1497.
[79] R.B. Jackson and W.E. Streib, Inorg. Chem., 10 (1971) 1760.
[80] R.T. Carlin and R.E. McCarley, Inorg. Chem., 28 (1989) 2604.
[81] J. San Filippo and M.A. Schaefer King, Inorg. Chem., 15 (1976) 1228.
[82] F.A. Cotton and B.J. Kalbacher, Inorg. Chem., 15 (1976) 522.
[83] J.M. Ball, P.M. Boorman and K.J. Moynihan, Can. J. Chem., 68 (1989) 685.
[84] P.M. Boorman, X. Gao, H. Jacobsen, H.-B. Kraatz, M. Parvez and T. Ziegler, Prepr. Div. Petrol. Chem., 206th Nat. Meet., American Chemical Society, Washington, DC, 1993, p. 6517.
[85] L. Messerle, Chem. Rev., 88 (1988) 1229.
[86] M.D. Fryzuk and D.H. McConville, Inorg. Chem., 28 (1989) 1613.
[87] R. Saillant and R.D.A. Wentworth, J. Am. Chem. Soc., 91 (1969) 2174.
[88] P.M. Boorman, W.S. Bell, K. Chong and X. Gao, Prepr. 11th Can. Symp. on Catalysis, Chem. Inst. Canada, Ottawa, 1990, p. 358.